

Figure 2.1 Critical path steps in an EHV line design. (From Electric Power Research Institute, 1979. Used by permission. © 1979 Electric Power Research Institute.)

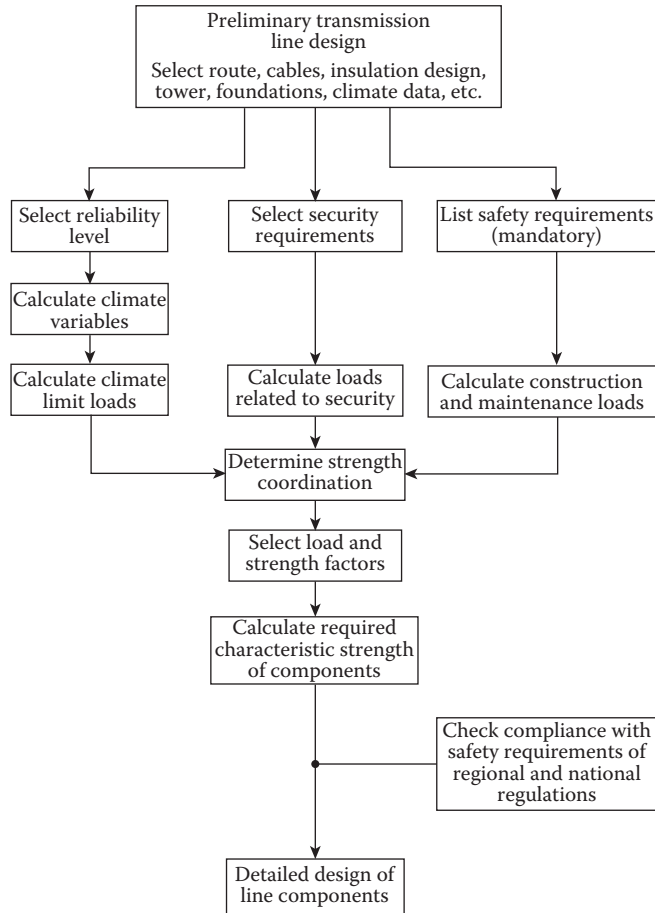


Figure 2.2 The methodology involved in developing improved design criteria of OH transmission lines based on reliability concepts.

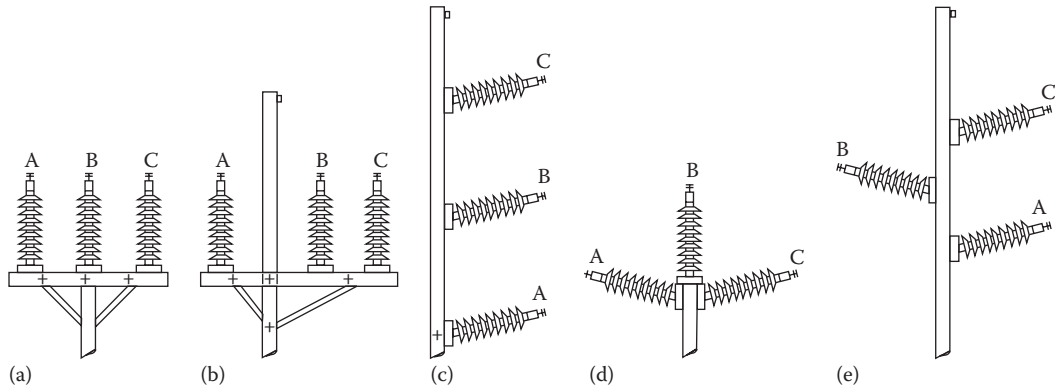


Figure 2.3 Typical compact configurations (not to scale): (a) horizontal unshielded, (b) horizontal shielded, (c) vertical, (d) delta, and (e) vertical delta. (From Electric Power Research Institute, *Transmission Line Reference Book: 115–138 kV Compact Line Design*, 2nd edn., EPRI, Palo Alto, CA, 1978. Used by permission. © 1978 Electric Power Research Institute.)

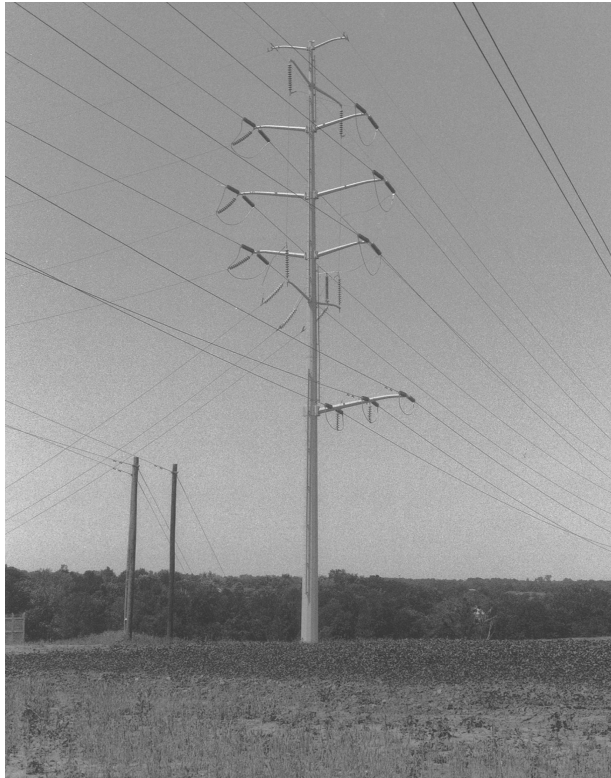


Figure 2.4 A double-circuit 138 kV line built by using steel poles, having two 138 kV top circuits and a 34.5 kV single circuit underbuilt. (Courtesy of Union Electric Company.)

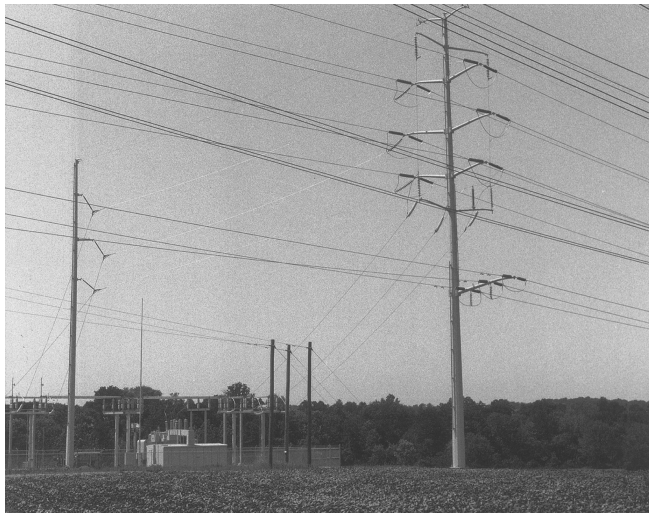


Figure 2.5 A double-circuit 138 kV line built by using steel poles, having two 138 kV top circuits and a 34.5 kV single circuit underbuilt. (Union Electric Company.)



Figure 2.6 A double-circuit 138 kV line built by using steel poles, having two 138 kV circuits underbuilt. (Union Electric Company.)

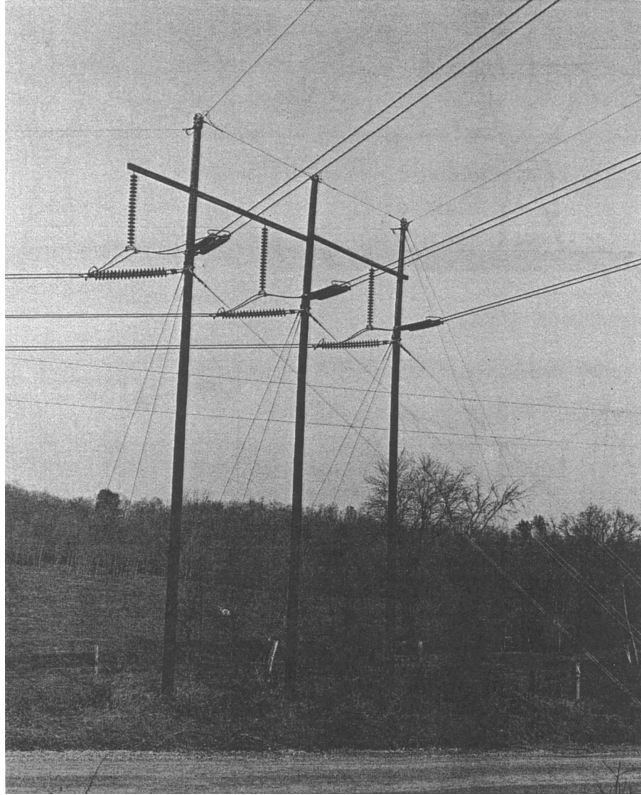


Figure 2.7 A typical 345 kV transmission line with single-circuit and wood H-frame. (Union Electric Company.)



Figure 2.8 A typical 345 kV transmission line with bundled conductors and double circuit on steel towers. (Union Electric Company.)

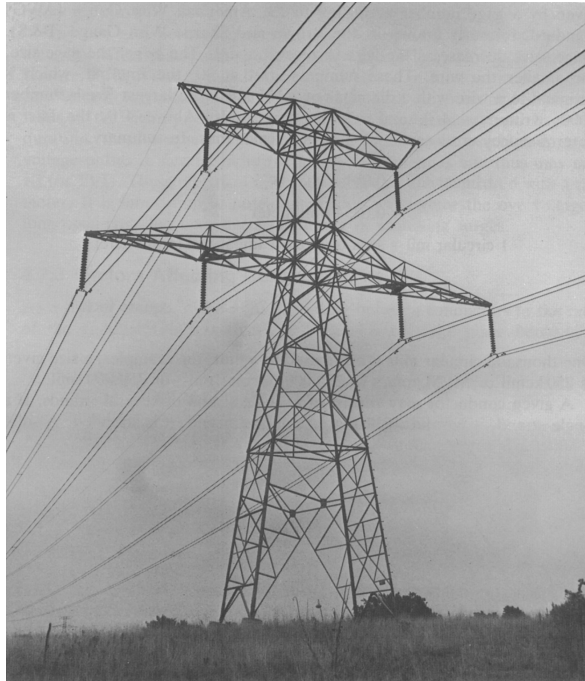


Figure 2.9 A typical 345 kV transmission line with bundled conductors and double circuit on steel towers. (Union Electric Company.)

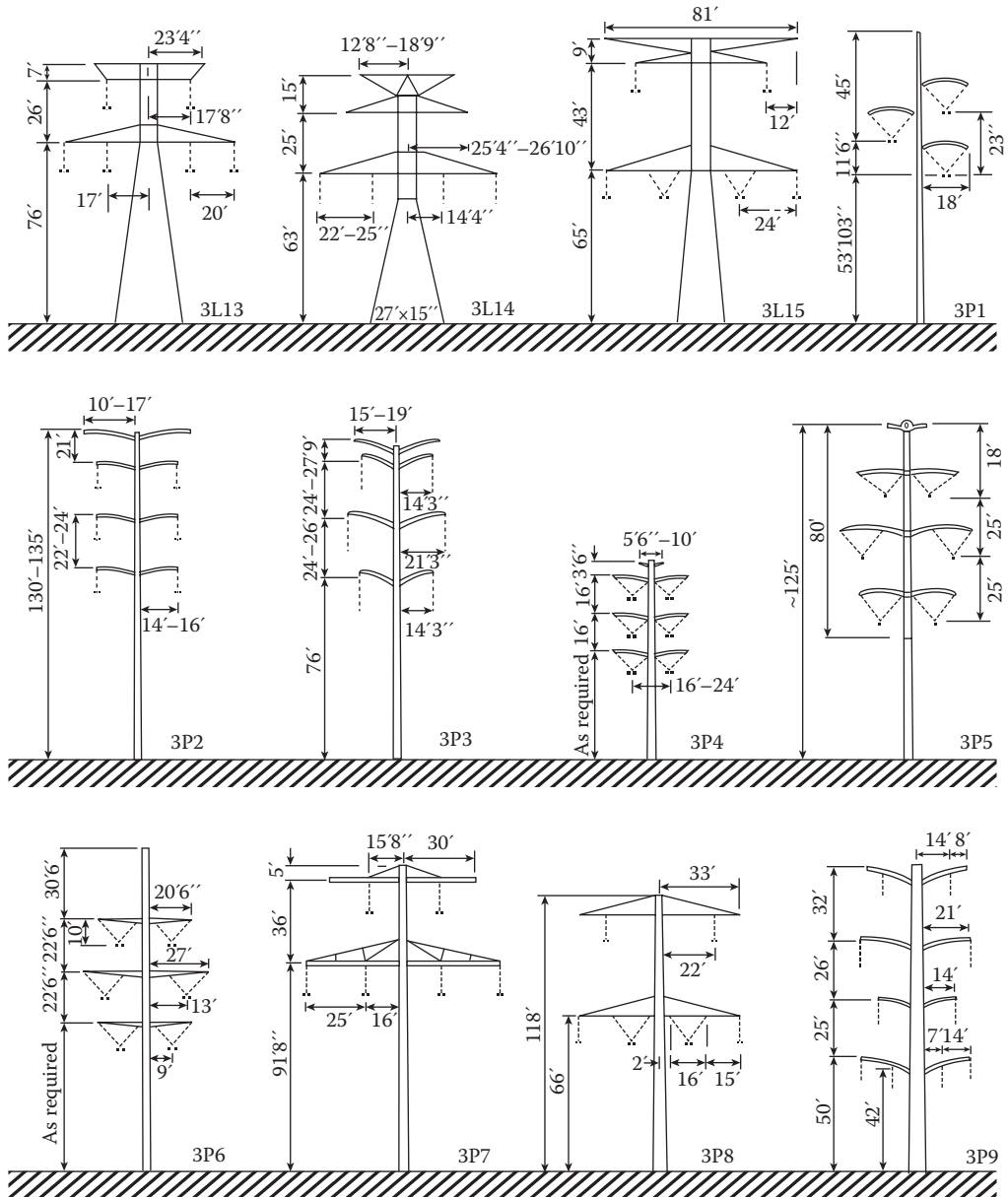


Figure 2.10 Typical pole- and lattice-type structures for 345 kV transmission systems. (From Electric Power Research Institute, *Transmission Line Reference Book: 345 kV and Above*, 2nd edn., EPRI, Palo Alto, CA, 1982. Used with permission. © 1979 Electric Power Research Institute.)

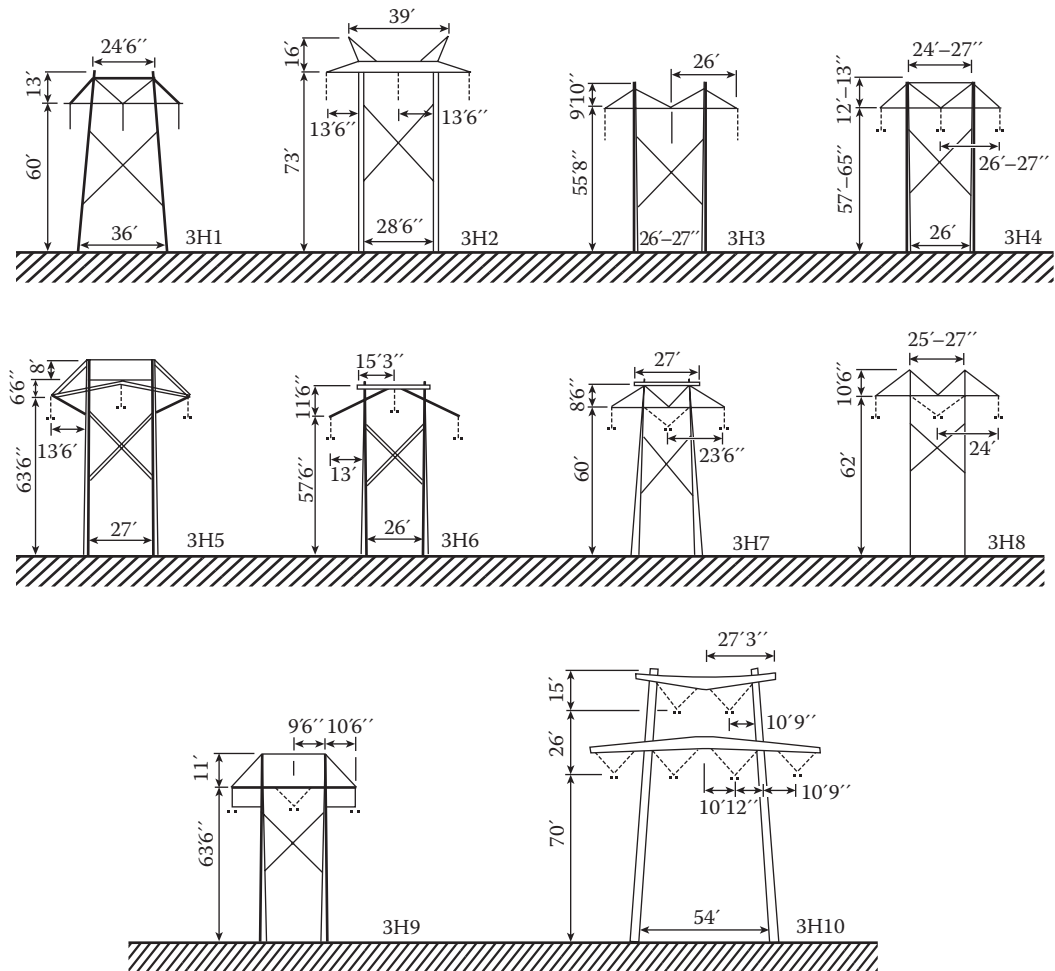


Figure 2.11 Typical wood H-frame-type structures for 345 kV transmission systems. (From Electric Power Research Institute, *Transmission Line Reference Book: 345 kV and Above*, 2nd edn., EPRI, Palo Alto, CA, 1982. Used by permission. © 1979 Electric Power Research Institute.)

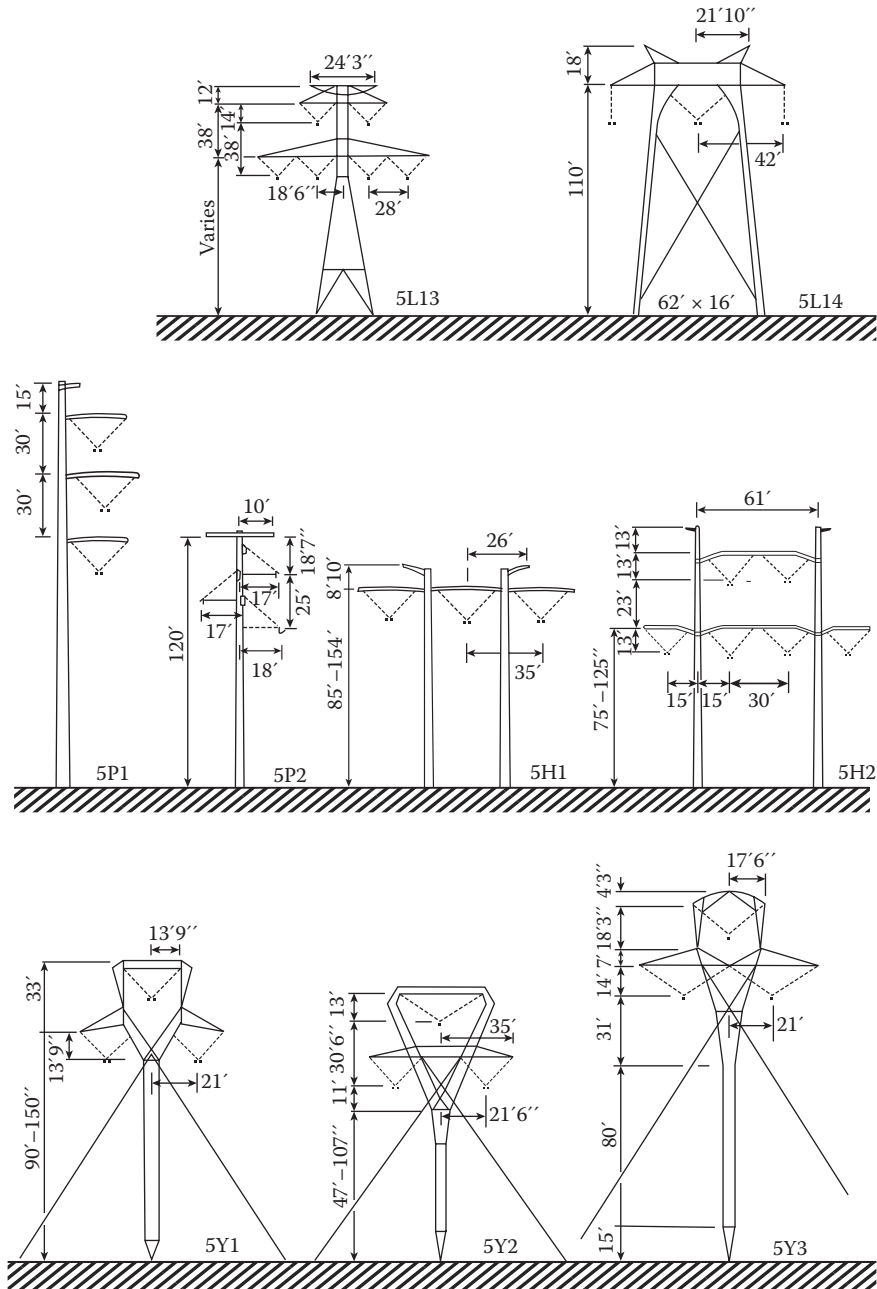


Figure 2.12 Typical pole- and lattice-type structures for 500 kV transmission systems. (From Electric Power Research Institute, *Transmission Line Reference Book: 345 kV and Above*, 2nd edn., EPRI, Palo Alto, CA, 1982. Used by permission. © 1979 Electric Power Research Institute.)

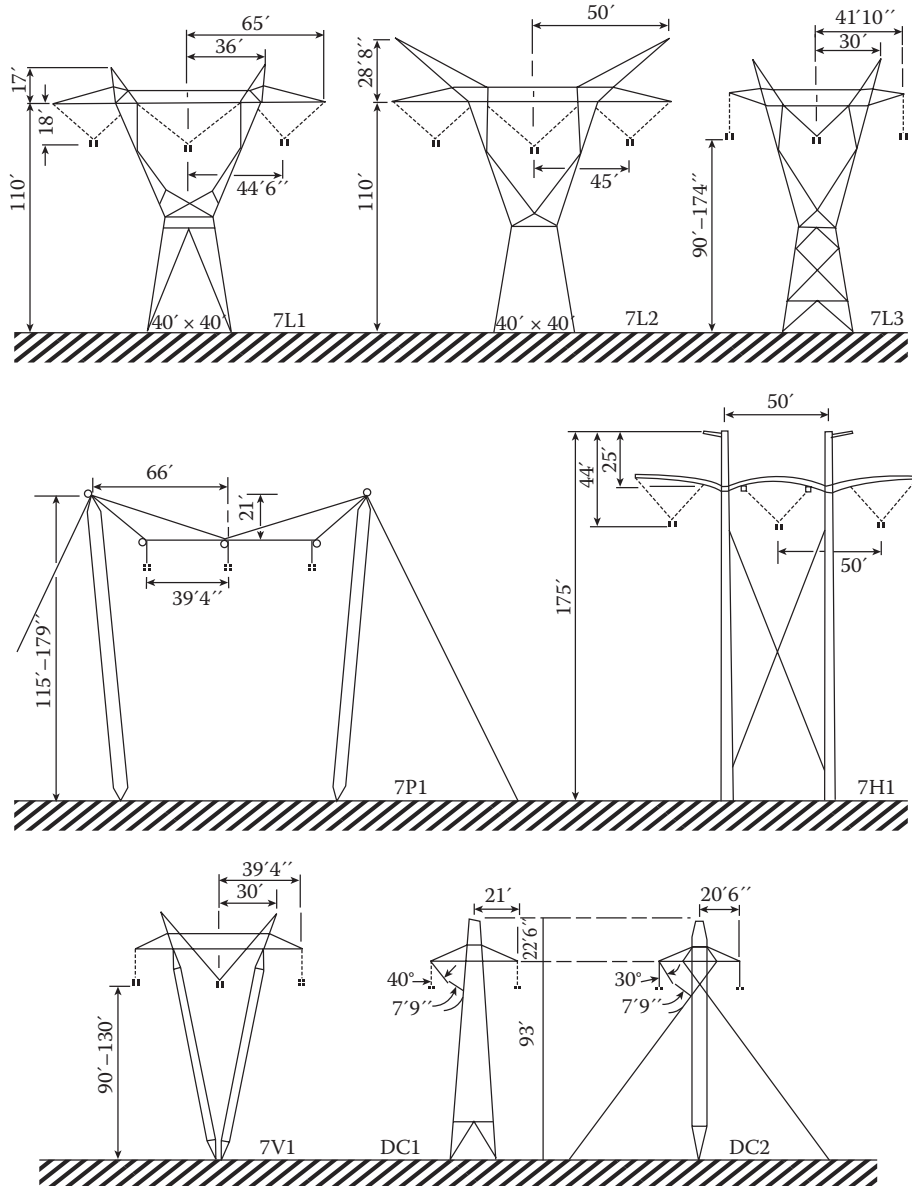


Figure 2.13 Typical pole- and lattice-type structures for 735–800 kV transmission systems. (From Electric Power Research Institute, *Transmission Line Reference Book: 345 kV and Above*, 2nd edn., EPRI, Palo Alto, CA, 1982. Used by permission. © 1979 Electric Power Research Institute.)



Figure 2.14 A typical 230 kV transmission line steel tower with bundled conductors and double circuit.



Figure 2.15 A lineman working from a helicopter platform.



Figure 2.16 Two 345 and 230 kV transmission lines side by side. (Courtesy of West Power Inc.)



Figure 2.17 A 345 kV transmission line and a 230 kV transmission line side by side. (Courtesy of West Power Inc.)



Figure 2.18 A 230/161 kV substation with a 230 kV transmission line passing by. (Courtesy of West Power Inc.)



Figure 2.19 A 115 kV transmission line and a 230 kV transmission line side by side. (Courtesy of West Power Inc.)



Figure 2.20 A cluster of four transmission lines side by side. (Courtesy of West Power Inc.)



Figure 2.21 A 115 kV transmission line and a 345 kV transmission line with corner towers. (Courtesy of West Power Inc.)



Figure 2.22 A 345 kV transmission line and a 115 kV transmission line side by side. (Courtesy of West Power Inc.)



Figure 2.23 A 230 kV switchyard. (Courtesy of West Power Inc.)



Figure 2.24 A pole-top view. (Courtesy of West Power Inc.)



Figure 2.25 A 230/34.5 kV switchyard. (Courtesy of West Power Inc.)



Figure 2.26 A galvanized dead-end corner pole of a 230 kV transmission line. (Courtesy of West Power Inc.)



Figure 2.27 A substation connection of transmission lines. (Courtesy of West Power Inc.)

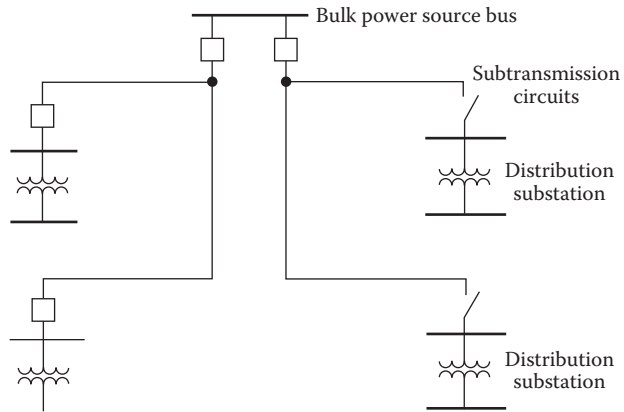


Figure 2.28 A radial-type subtransmission. (Courtesy of West Power Inc.)

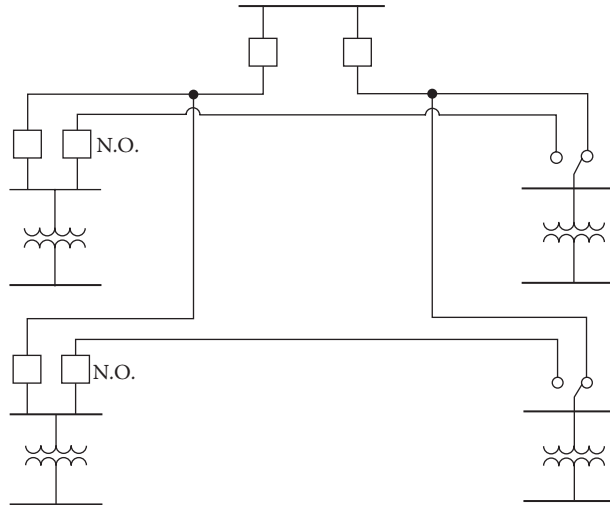


Figure 2.29 An improved form of radial-type subtransmission. (Courtesy of West Power Inc.)

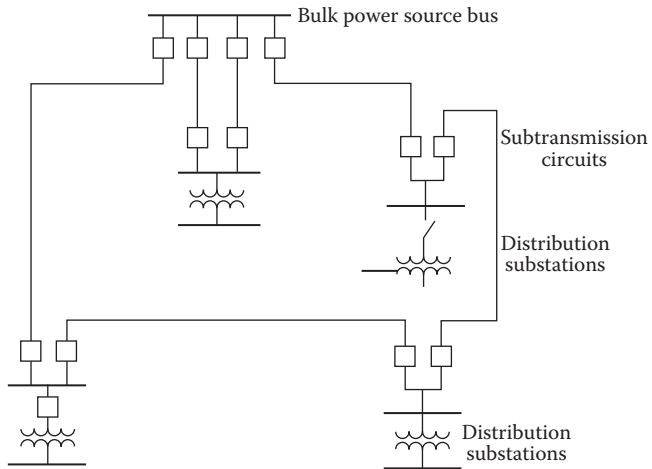


Figure 2.30 A loop-type subtransmission.





Figure 2.32 A typical 34.5 kV line with a double circuit and wood poles. It has a newer style construction. (Union Electric Company.)



Figure 2.33 A 34.5 kV line with a single circuit and wood poles. It also has a 12.47 kV underbuilt line and 34.5 kV switch. It has an old style construction. (Union Electric Company.)



Figure 2.34 A typical 34.5 kV line with a double circuit and wood poles. It also has a 4.16 kV underbuilt line and a 34.5 kV switch. (Union Electric Company.)

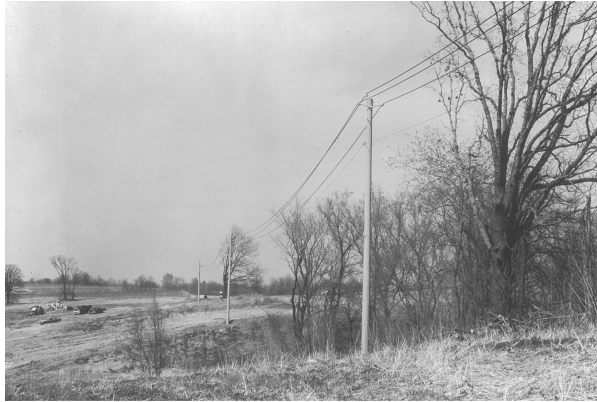


Figure 2.35 A typical 12.47 kV line with a single circuit and wood pole. It has a newer type of pole-top construction. (Union Electric Company.)

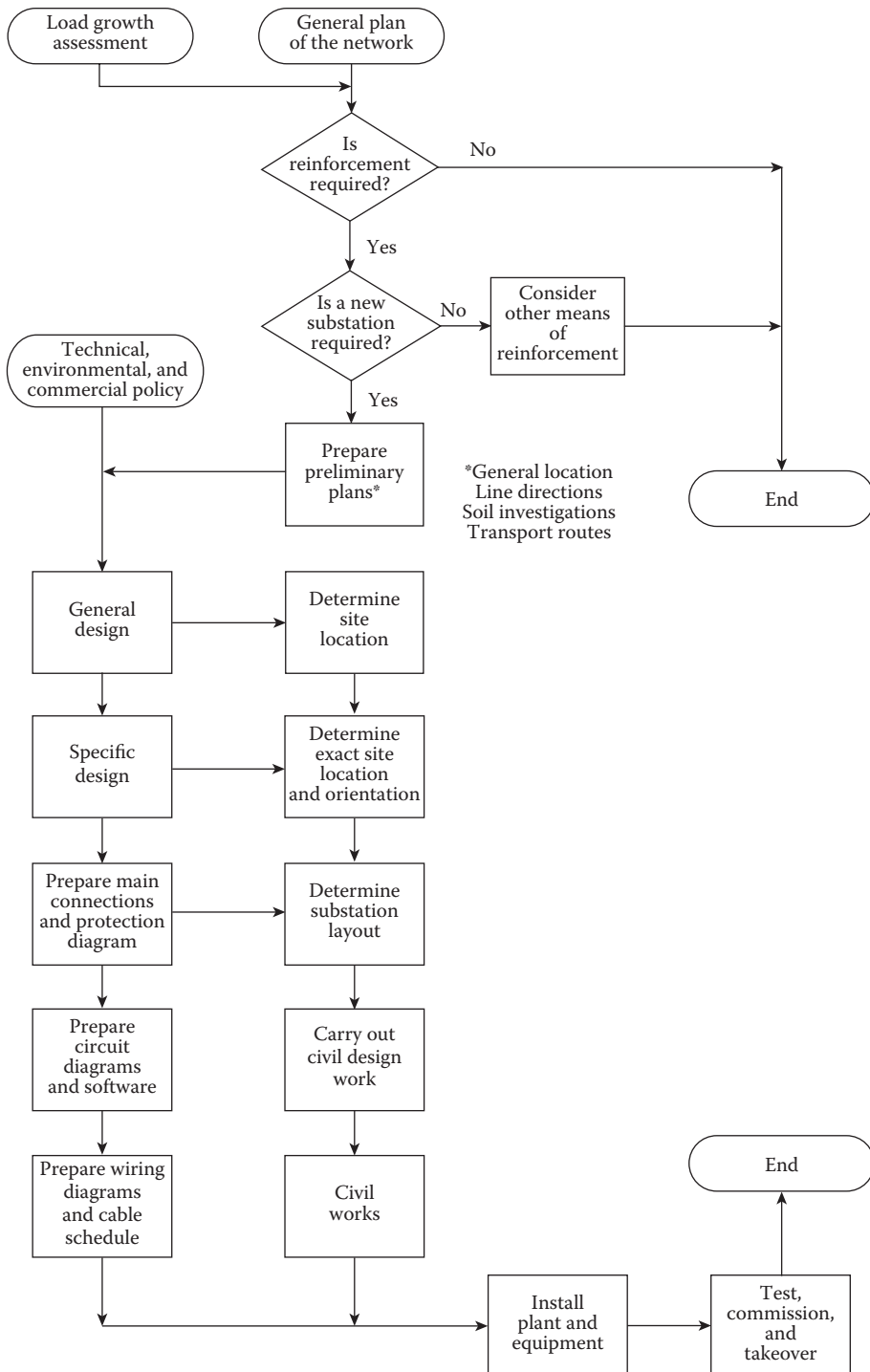


Figure 2.36 Establishment of a new substation. (From Burke, J. and Shazizian, M., How a substation happens?, in *Electric Power Substation Engineering*, J. D. McDonald, ed., CRC Press, Boca Raton, FL, 2007.)



Figure 2.37 A bulk power substation operating at 138/34.5 kV voltage level. (Union Electric Company.)

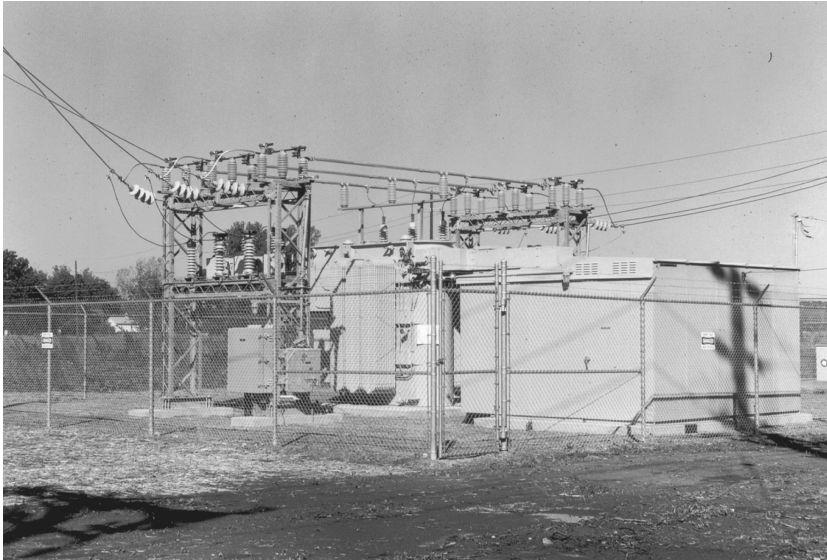


Figure 2.38 A distribution substation operating at 34.5/12.47 kV voltage level. (Union Electric Company.)

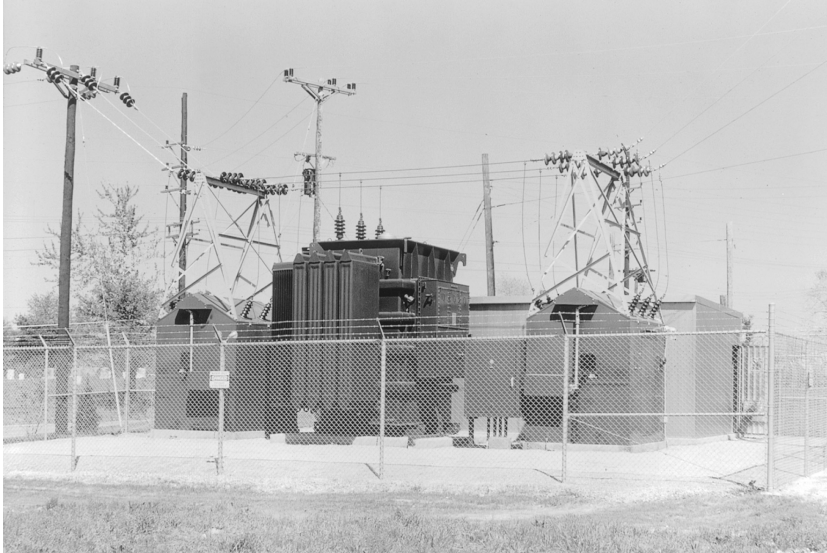


Figure 2.39 A distribution substation operating at 34.5/4.16 kV voltage level. (Union Electric Company.)

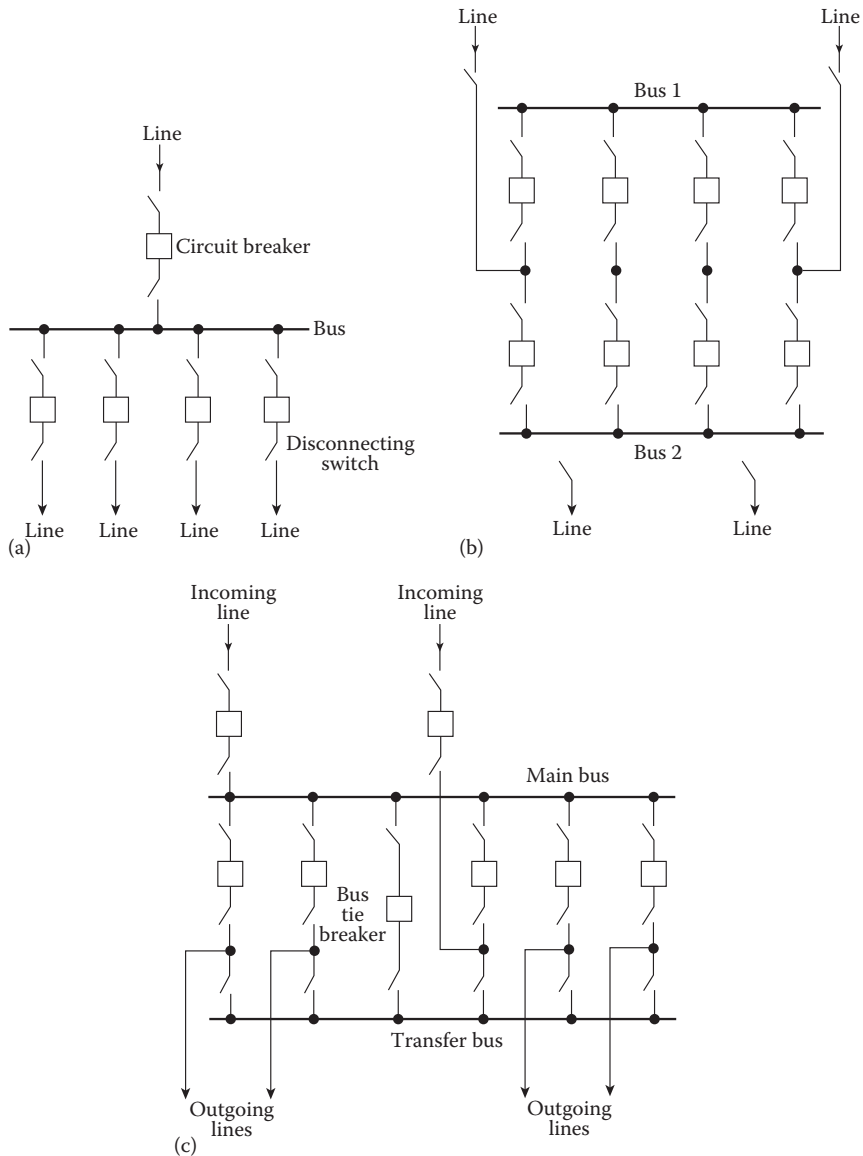


Figure 2.40 Most commonly used substation bus schemes: (a) single-bus scheme, (b) double-bus-double-breaker scheme, and (c) main-and-transfer bus scheme.

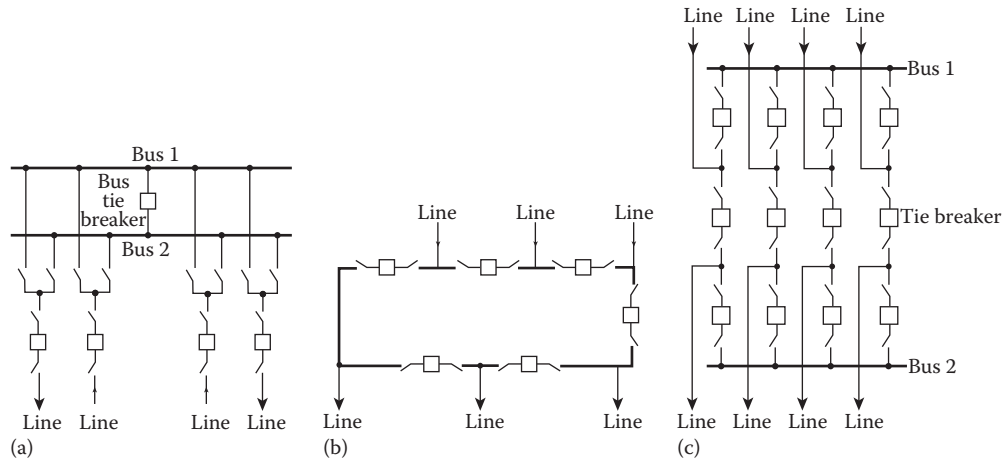


Figure 2.41 Most commonly used substation bus schemes: (a) double-bus–single-breaker scheme, (b) ring bus scheme, and (c) breaker-and-a-half scheme.

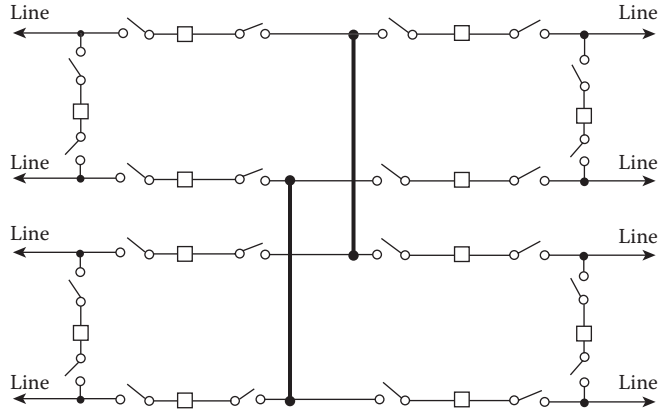


Figure 2.42 A low-profile EHV substation using inverted breaker-and-a-half scheme.

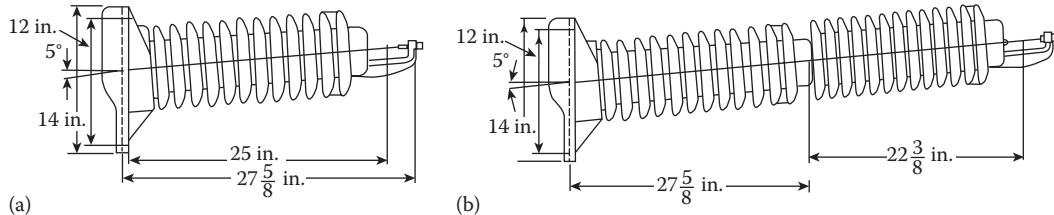


Figure 2.43 Typical (side) post-type insulators used in (a) 69 kV and (b) 138 kV.

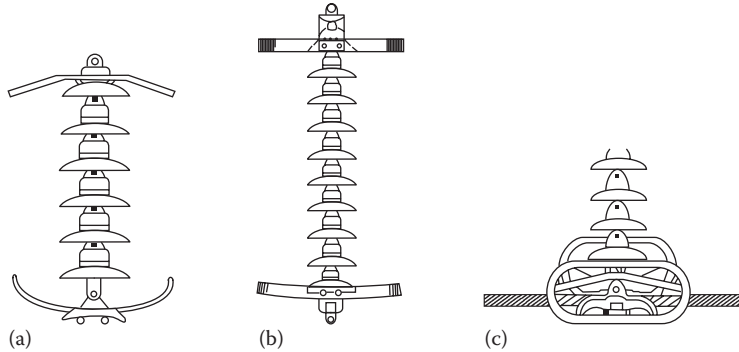


Figure 2.44 Devices used to protect insulator strings: (a) suspension string with arcing horns, (b) suspension string with grading shields (or *arcing rings*), and (c) suspension string with control ring. (Courtesy of The Ohio Brass Company.)

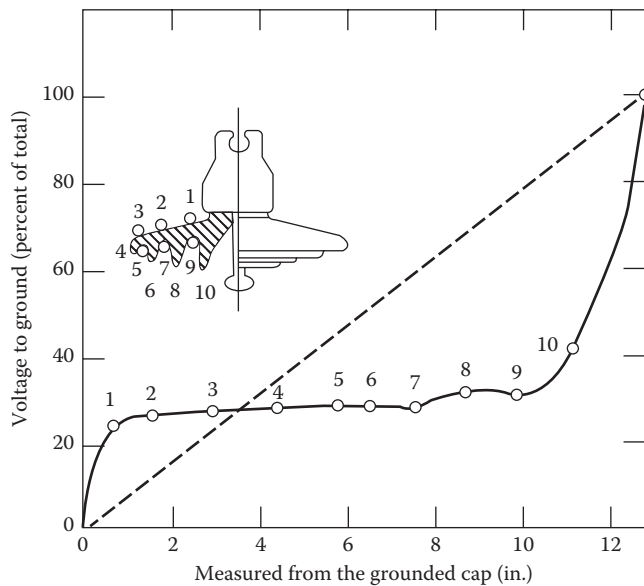


Figure 2.45 Voltage distribution along the surface of single clean cap-and-pin suspension insulator.

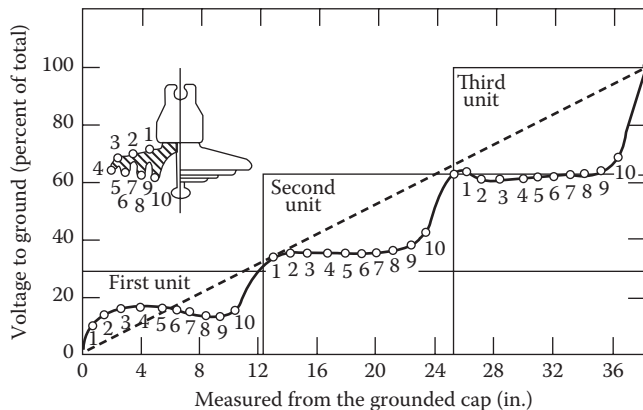


Figure 2.46 A typical voltage distribution on surfaces of three clean cap-and-pin suspension insulator units in series.

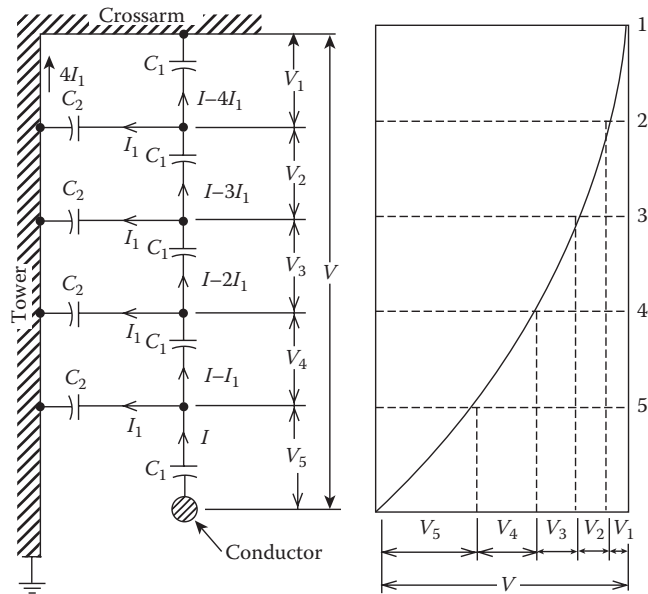


Figure 2.47 Voltage distribution among suspension insulator units.

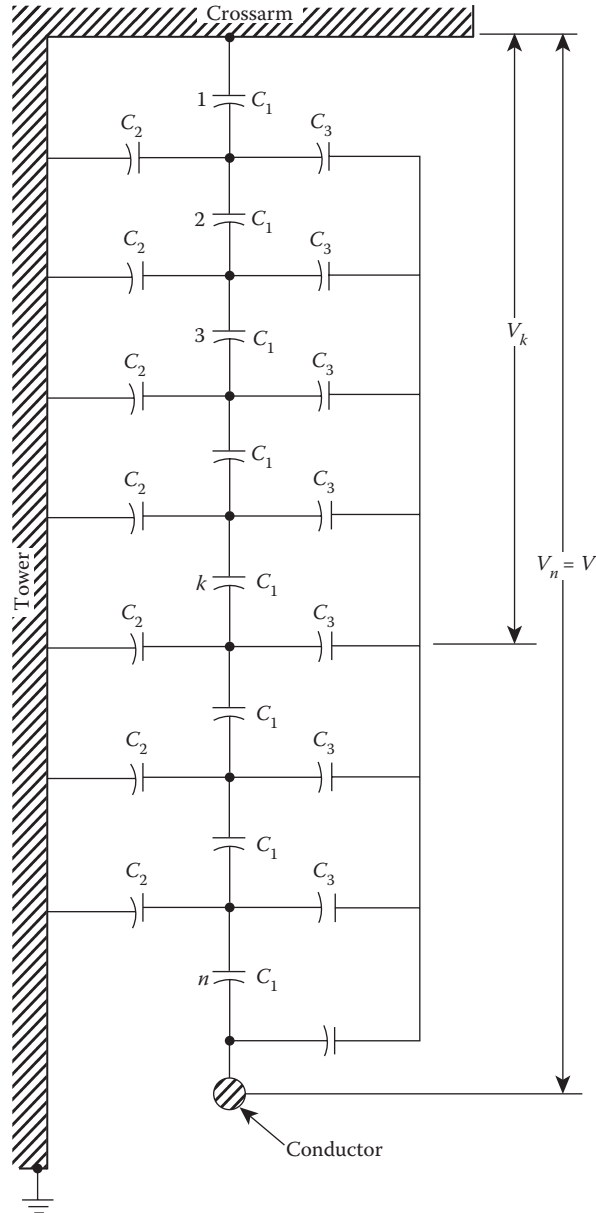


Figure 2.48 An equivalent circuit for voltage distribution along clean eight-unit insulator string. (Adopted from Edison Electric Institute, *EHV Transmission Line Reference Book*, EEI, New York, 1968.)

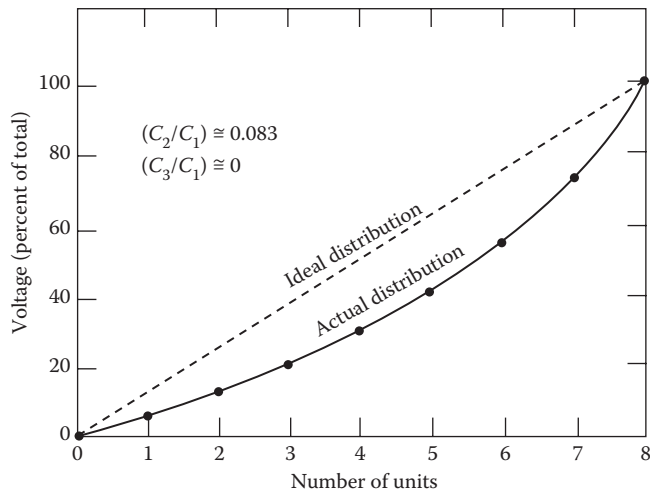


Figure 2.49 Voltage distribution along a clean eight-unit cap-and-pin insulator string.

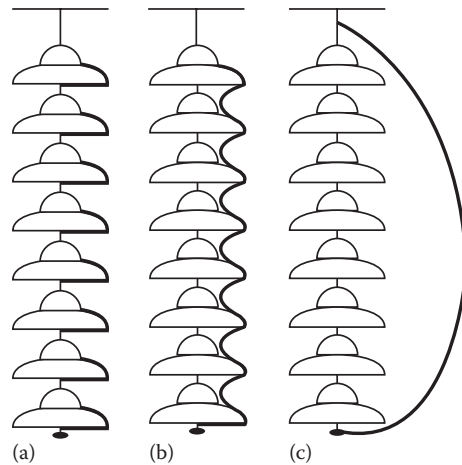


Figure 2.50 Changes in channel position of contaminated flashover.

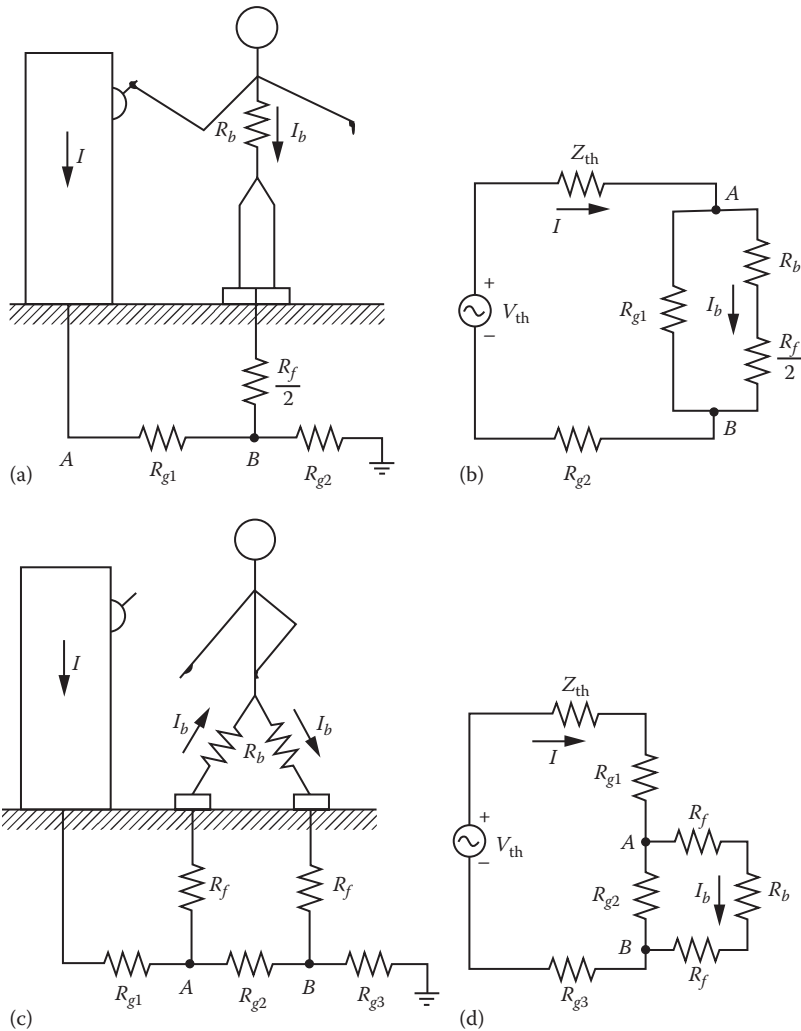


Figure 2.51 Typical electrical shock hazard situations: (a) touch potential, (b) its equivalent circuit, (c) step potential, and (d) its equivalent circuit.

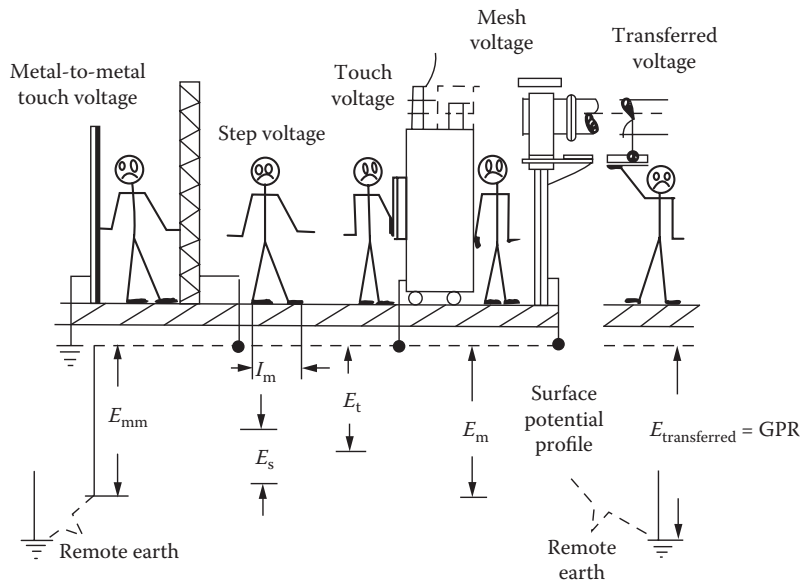


Figure 2.52 Possible basic shock situations. (From Keil, R.P., Substation grounding, in *Electric Power Substation Engineering*, Chapter 11, Figure 11.6, CRC Press, Boca Raton, FL, 2003, pp. 11-7. With permission.)

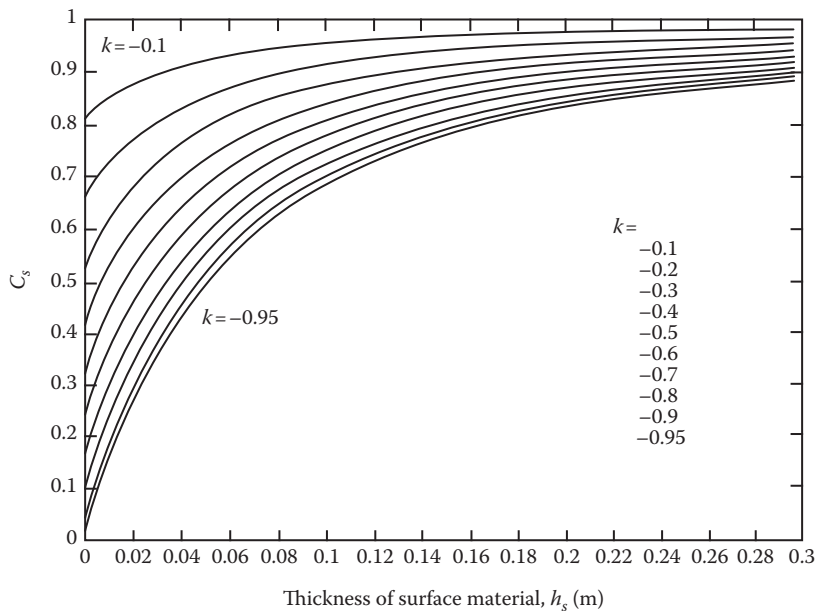


Figure 2.53 Surface layer derating factor C_s versus thickness of surface material in meters. (From From Keil, R.P., Substation grounding, in *Electric Power Substation Engineering*, Chapter 11, CRC Press, Boca Raton, FL, 2003. With permission.)

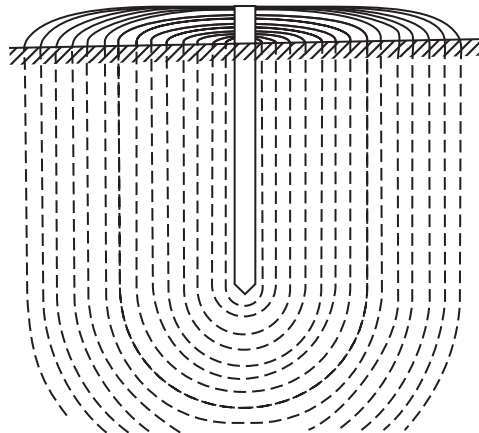


Figure 2.54 Resistance of earth surrounding an electrode.

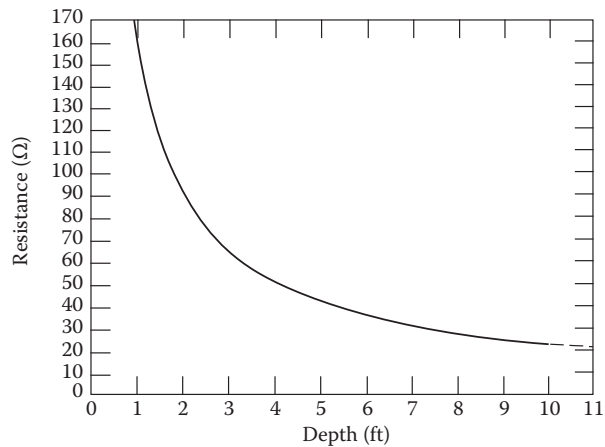


Figure 2.55 Variation of soil resistivity with depth for soil having uniform moisture content at all depths. (From National Bureau of Standards Technical Report 108.)

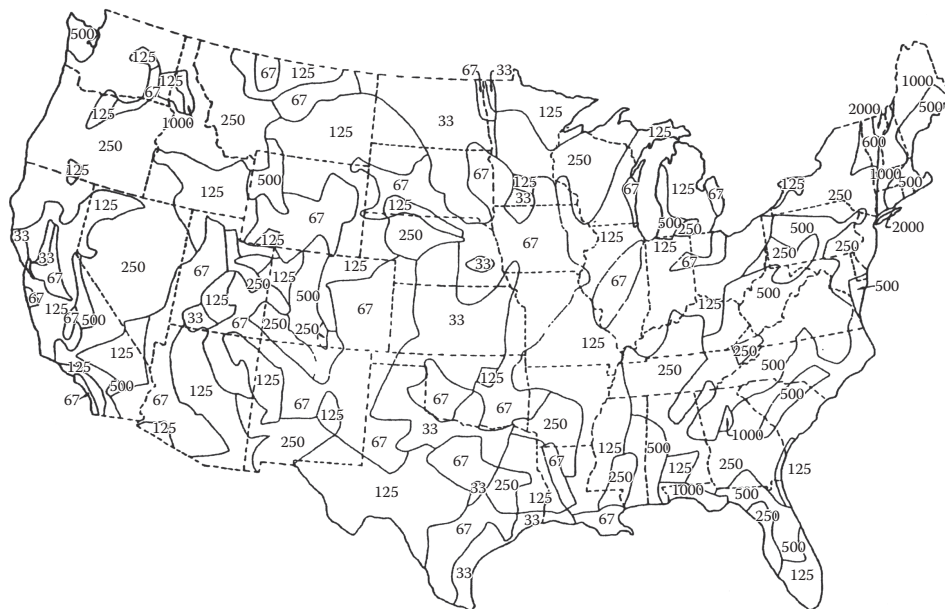


Figure 2.56 Approximate ground resistivity distribution in the United States. *Notes:* All figures on this map indicate ground resistivity (ρ) in ohm-meters. These data are taken from FCC figure M3, February 1954. The FCC data indicate ground conductivity in milliohms per meter. Resistivities of special note from Transmission Line Reference Book by EPRI in ohmmeters: Swampy ground (10–100), pure slate (10,000,000), and sandstone (100,000,000). (From Keil, R.P., Substation grounding, in *Electric Power Substation Engineering*, Chapter 11, CRC Press, Boca Raton, FL, 2003.)

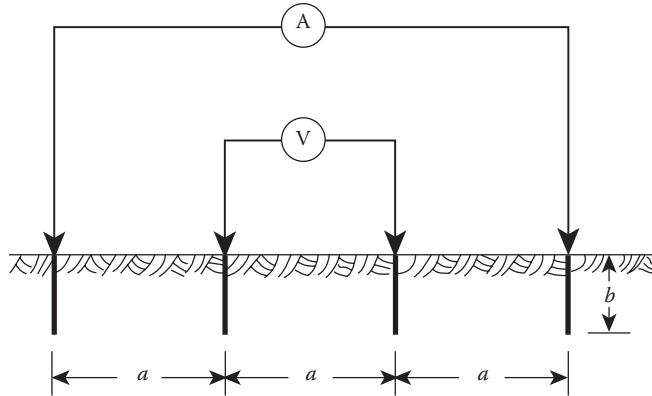


Figure 2.57 Wenner four-pin method.

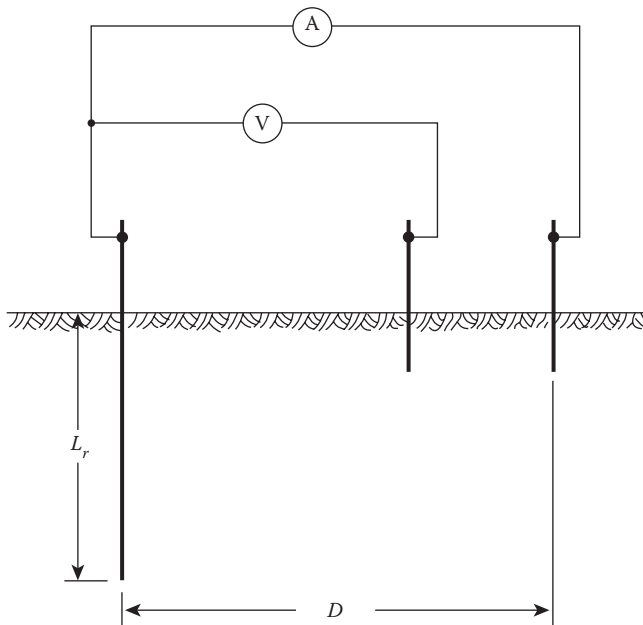


Figure 2.58 Circuit diagram for three-pin or driven-ground rod method.

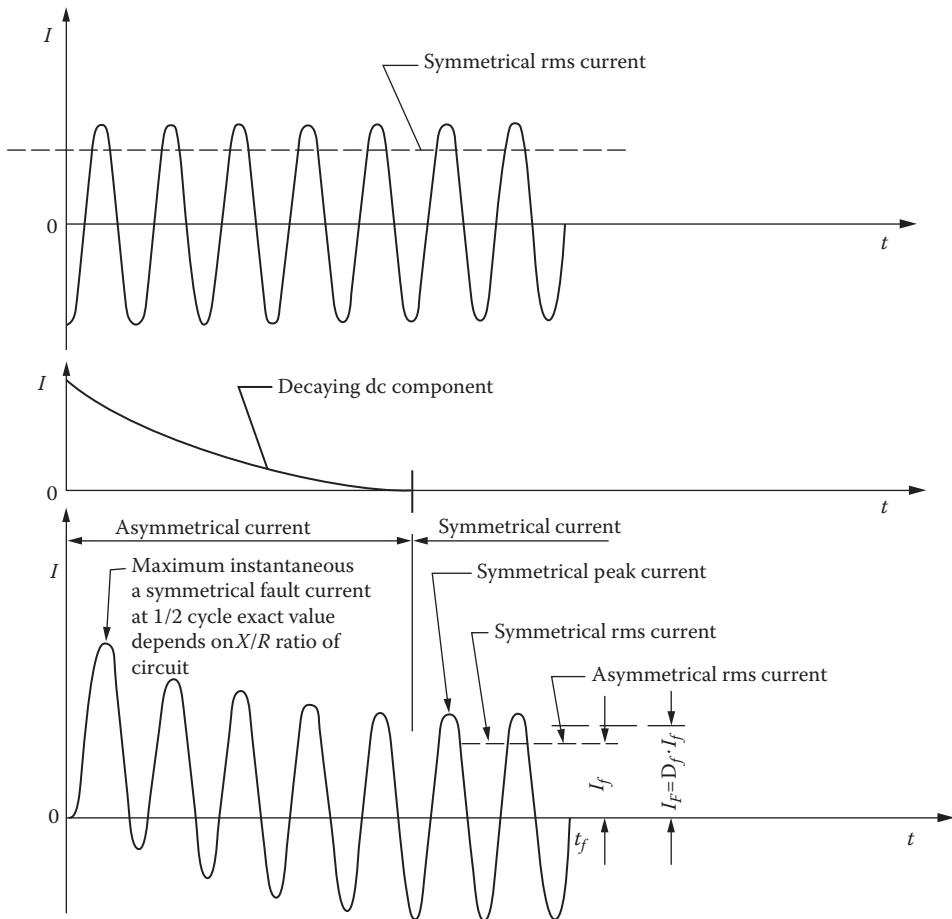


Figure 2.59 The relationship between asymmetrical fault current, dc decaying component, and symmetrical fault current.

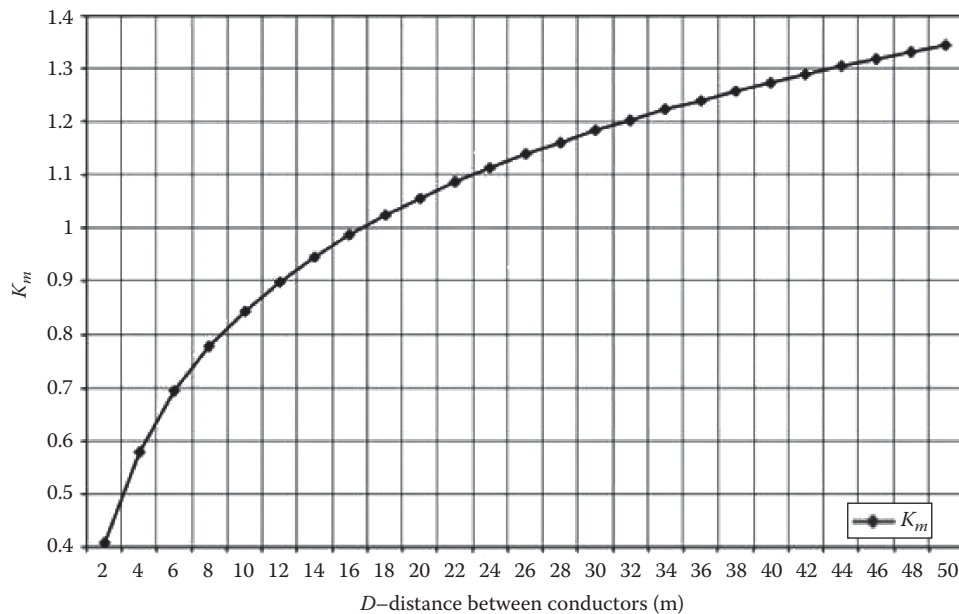


Figure 2.60 The effect of the spacing (D) between conductors on K_m . (From Keil, R.P., Substation grounding, in *Electric Power Substation Engineering*, Chapter 11, CRC Press, Boca Raton, FL, 2003. With permission.)

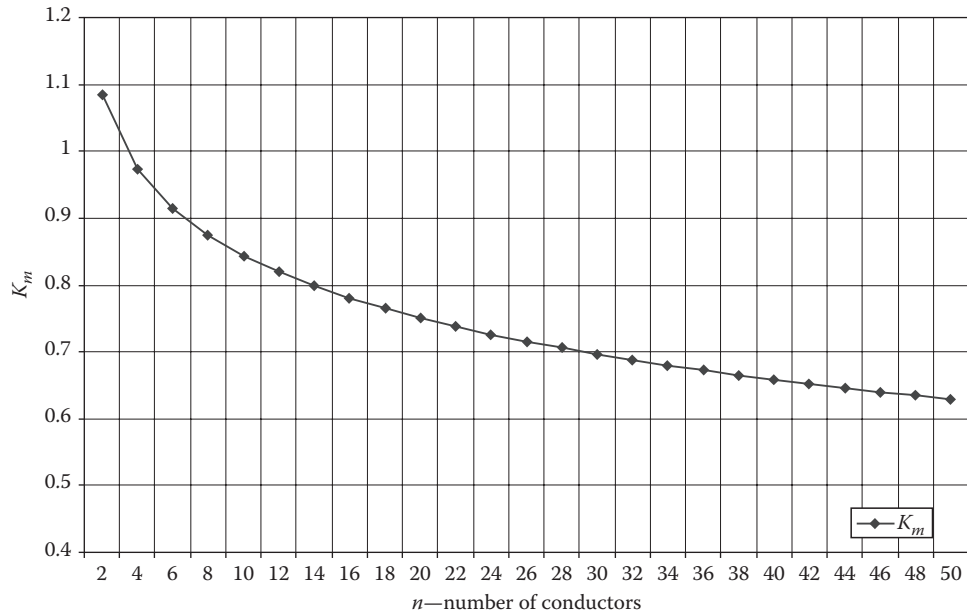


Figure 2.61 The effect of the number of conductors (n) on the K_m . (From Keil, R.P., Substation grounding, in *Electric Power Substation Engineering*, Chapter 11, CRC Press, Boca Raton, FL, 2003. With permission.)

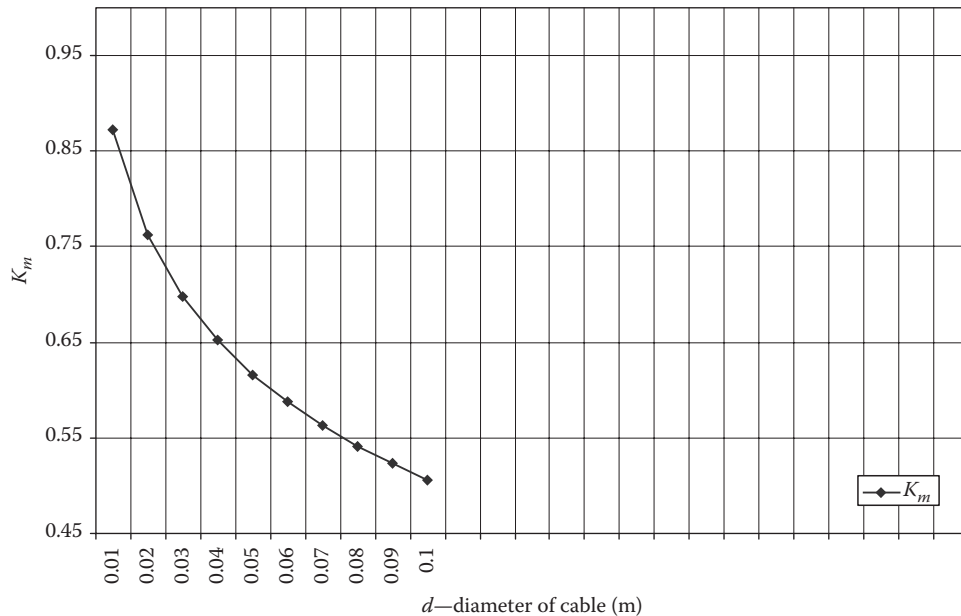


Figure 2.62 The relationship between the diameter of the conductor (d) and the K_m . (From Keil, R.P., Substation grounding, in *Electric Power Substation Engineering*, Chapter 11, CRC Press, Boca Raton, FL, 2003. With permission.)

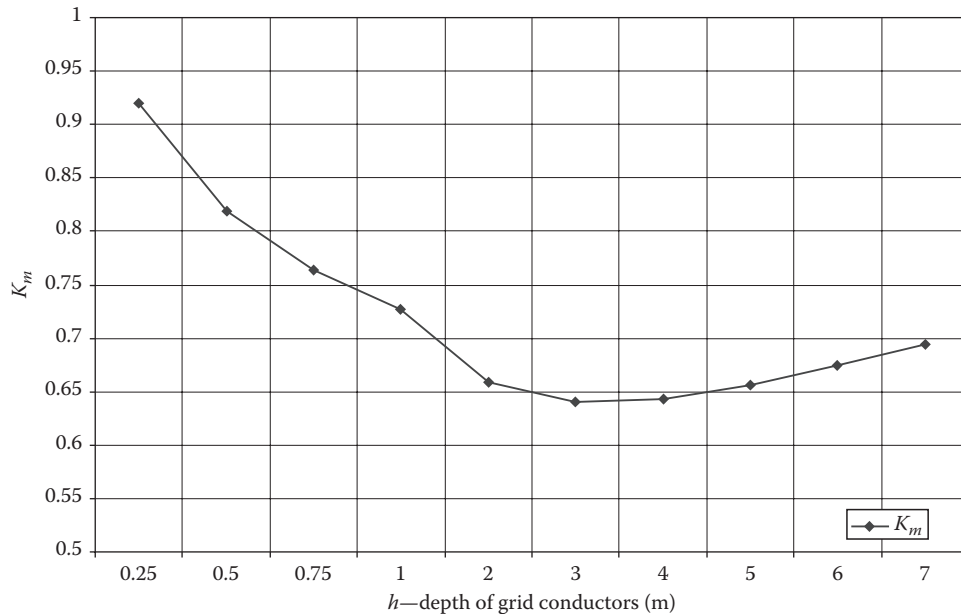


Figure 2.63 The relationship between the depth of the conductor (h) and K_m . (From Keil, R.P., Substation grounding, in *Electric Power Substation Engineering*, Chapter 11, CRC Press, Boca Raton, FL, 2003. With permission.)

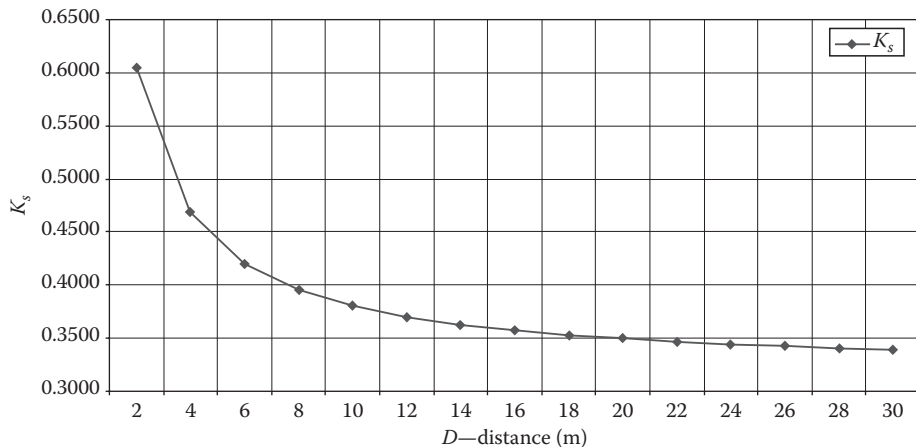


Figure 2.64 The relationship between the distance (D) between the conductors and the geometric factor K_s . (From Keil, R.P., Substation grounding, in *Electric Power Substation Engineering*, Chapter 11, CRC Press, Boca Raton, FL, 2003. With permission.)

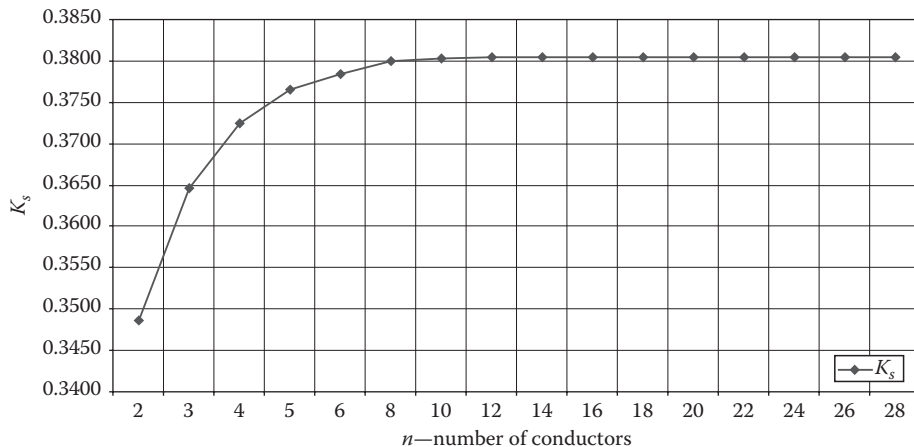


Figure 2.65 The relationship between the number of conductors (n) and the geometric factor K_s . (From Keil, R.P., Substation grounding, in *Electric Power Substation Engineering*, Chapter 11, CRC Press, Boca Raton, FL, 2003. With permission.)

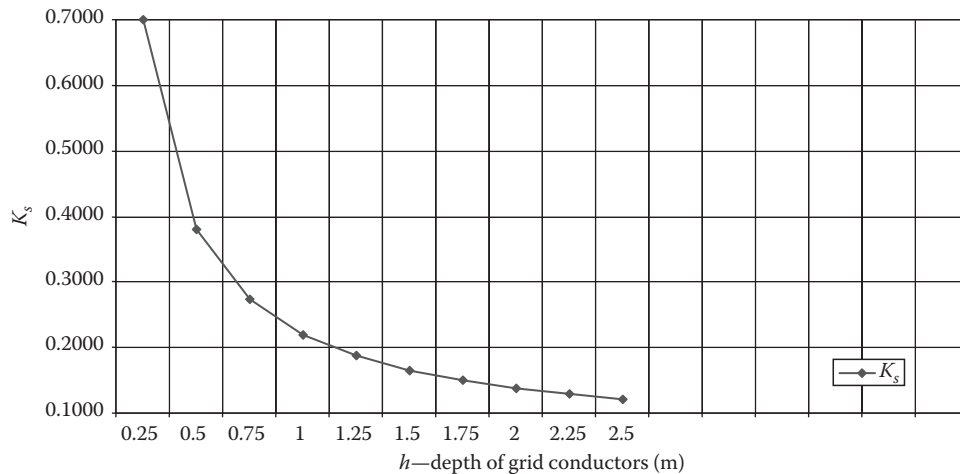


Figure 2.66 The relationship between the depth of grid conductors (h) in meter and the geometric factor K_s . (From Keil, R.P., Substation grounding, in *Electric Power Substation Engineering*, Chapter 11, CRC Press, Boca Raton, FL, 2003. With permission.)

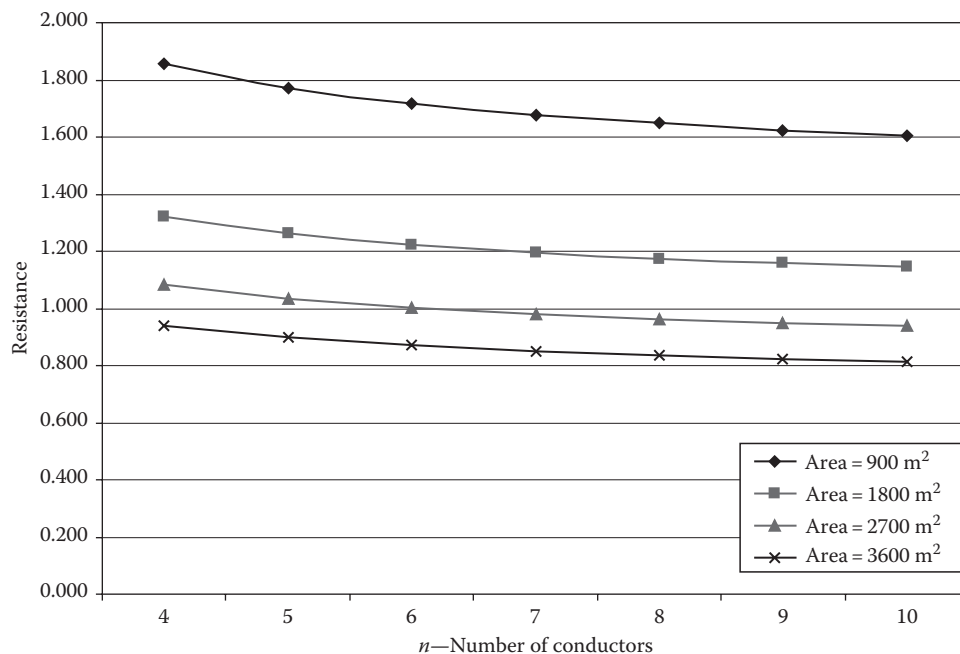


Figure 2.67 The effects of number of grid conductors (n), without ground rods, on the ground grid resistance.

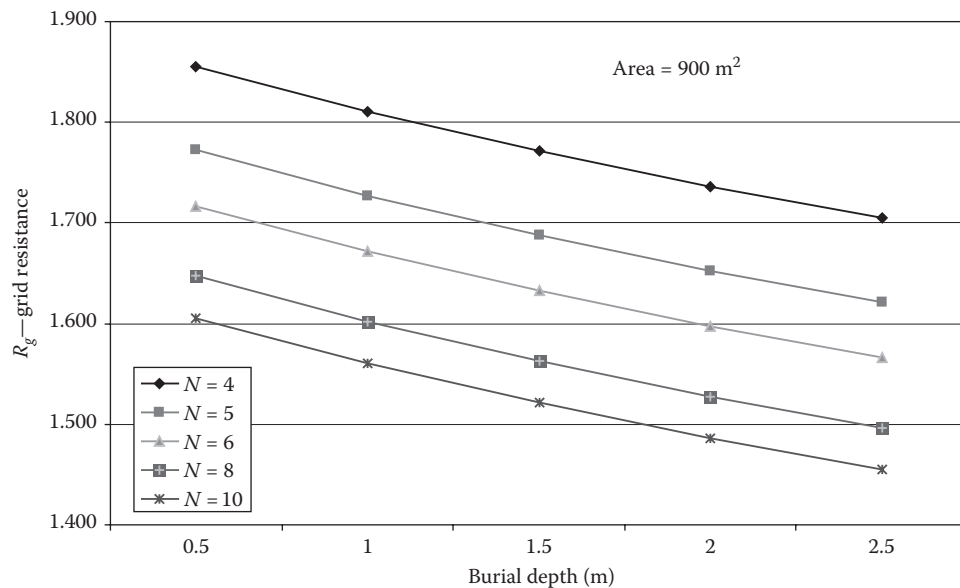


Figure 2.68 The effects of varying the depth of burial of the grid (h) from 0.5 to 2.5 m and the number of conductors from 4 to 10. (From Keil, R.P., Substation grounding, in *Electric Power Substation Engineering*, Chapter 11, CRC Press, Boca Raton, FL, 2003; Electric Power Research Institute, *Transmission Line Reference Book: 345 kV and Above*, 2nd edn., EPRI, Palo Alto, CA, 1982. With permission.)

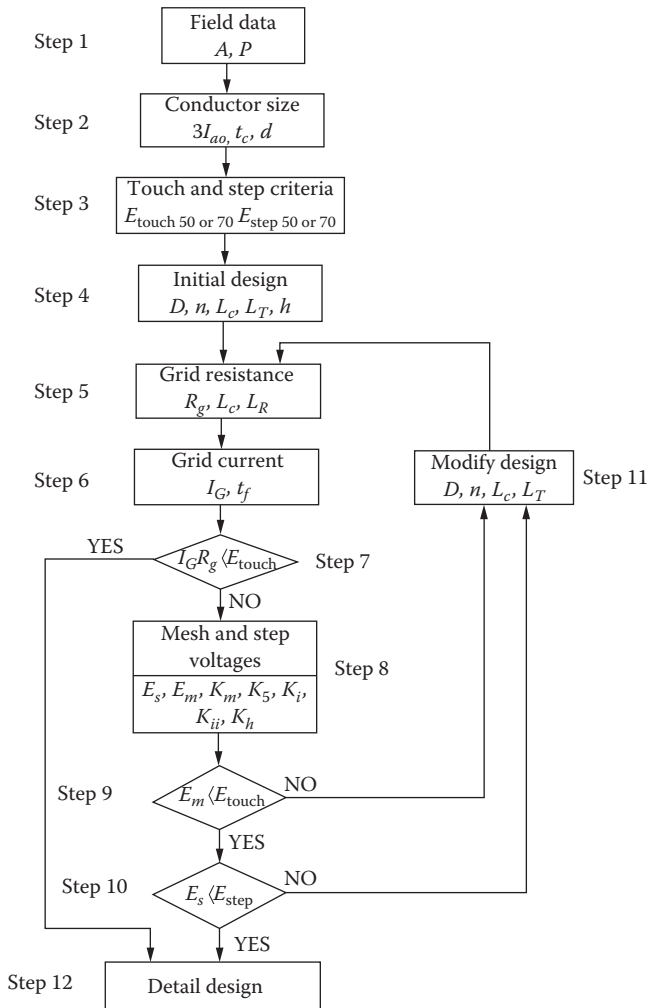


Figure 2.69 Substation grounding design procedure block diagram.

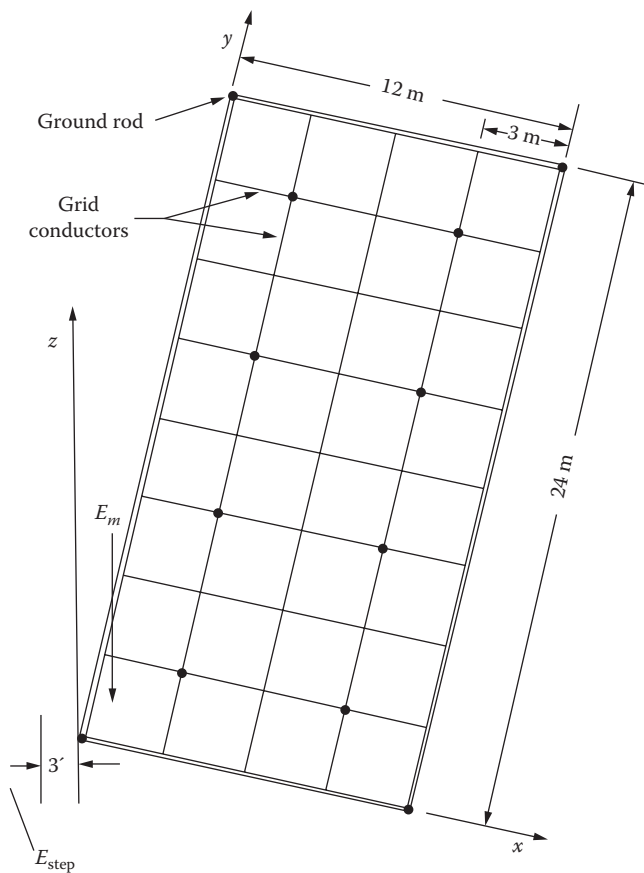


Figure 2.70 Preliminary design.

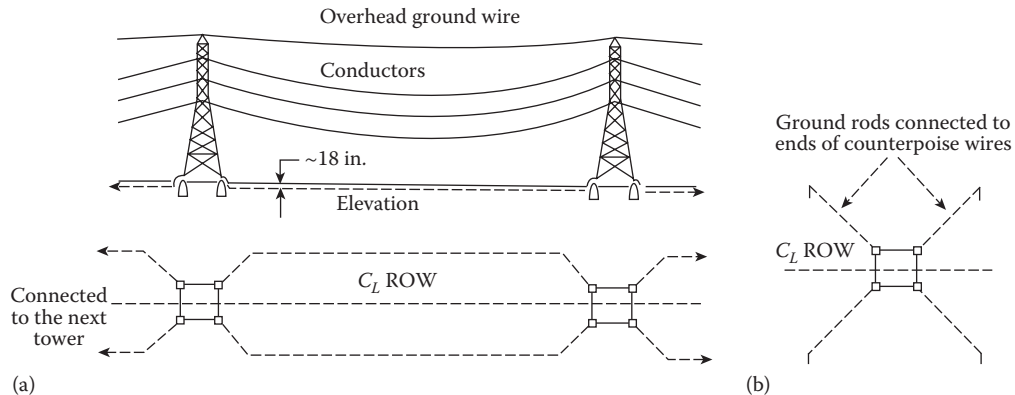


Figure 2.71 Two basic types of counterpoises: (a) continuous (parallel) and (b) radial.

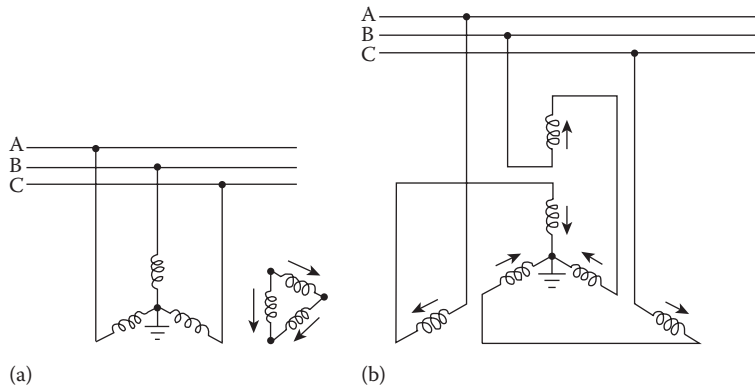


Figure 2.72 Grounding transformers used in delta-connected systems: (a) using wye–delta-connected small distribution transformers or (b) using grounding autotransformers with interconnected wye or *zigzag* windings.

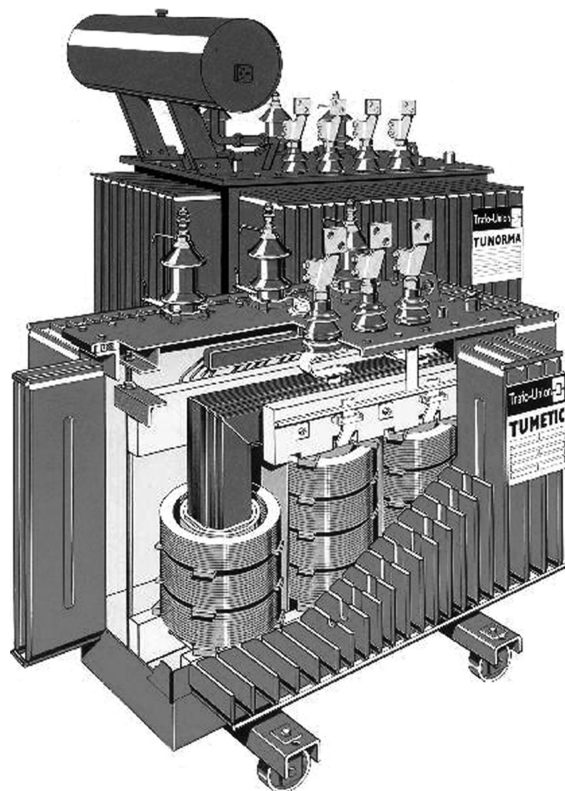


Figure 2.73 A 40 MVA, 110 kV $\pm 16\%/21$ kV, three-phase, core-type transformer, 5.2 m high, 9.4 m long, 3 m wide, weighing 80 tons. (Courtesy of Siemens AG.)

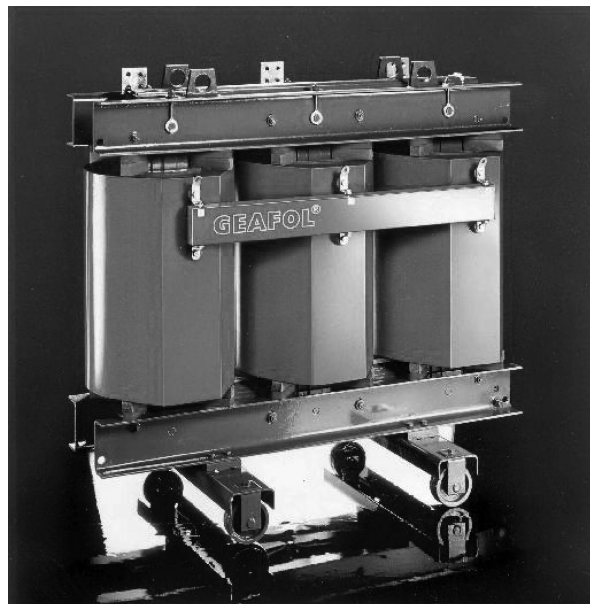


Figure 2.74 A 850/950/1100 MVA, 415 kV $\pm 11\%/27$ kV, three-phase, shell-type transformer, 11.3 high, 14 long, 5.7 wide, weighing (without cooling oil) 552 tons. (Courtesy of Siemens AG.)

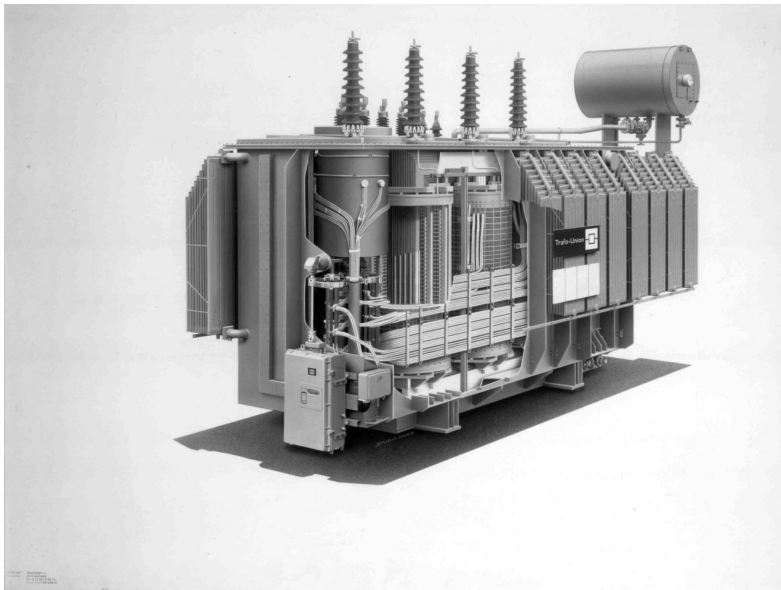


Figure 2.75 The 10 MVA and 50 kVA, core-type three-phase transformers with GEA FOL solid dielectric cores. (Courtesy of Siemens AG.)

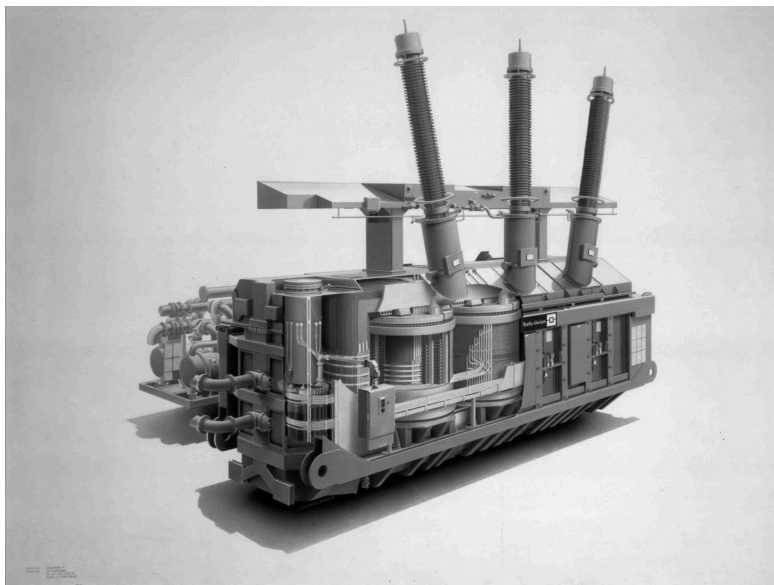


Figure 2.76 A typical core and coil assembly of a three-phase, core-type, power transformer. (Courtesy of Siemens AG.)

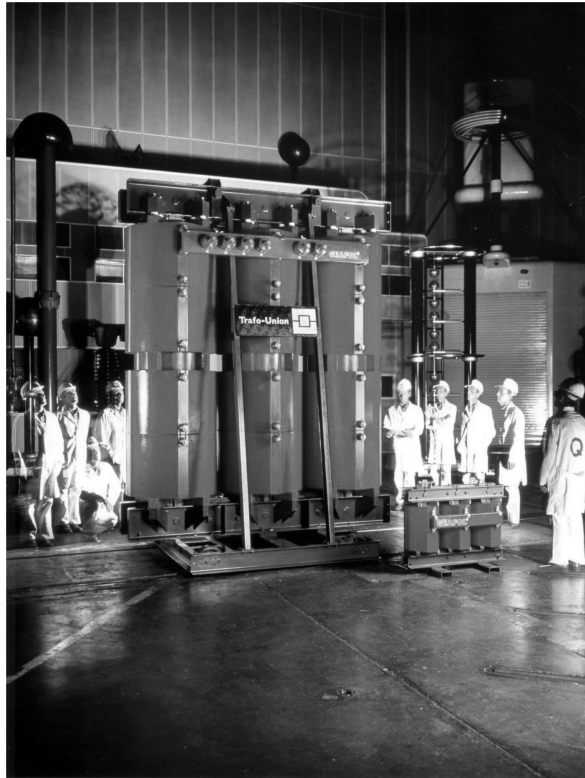


Figure 2.77 The 10MVA and 50 kVA, core-type three-phase transformers with GEAFOL solid dielectric cores. (Courtesy of Siemens AG.)

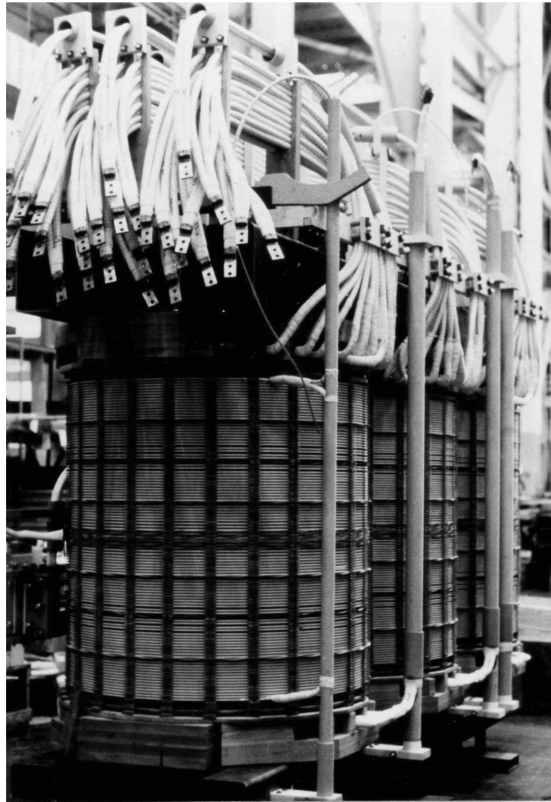


Figure 2.78 A core-type three-phase transformer with GEAFOL solid dielectric core. (Courtesy of Siemens AG.)

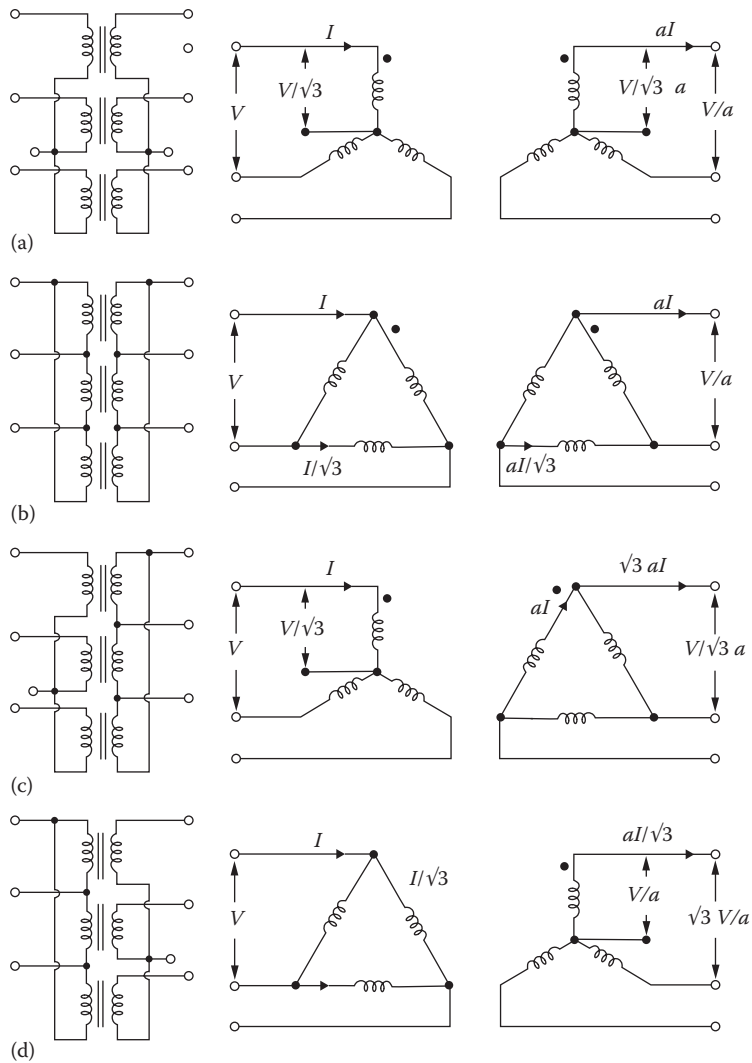


Figure 2.79 Possible three-phase transformer connections.

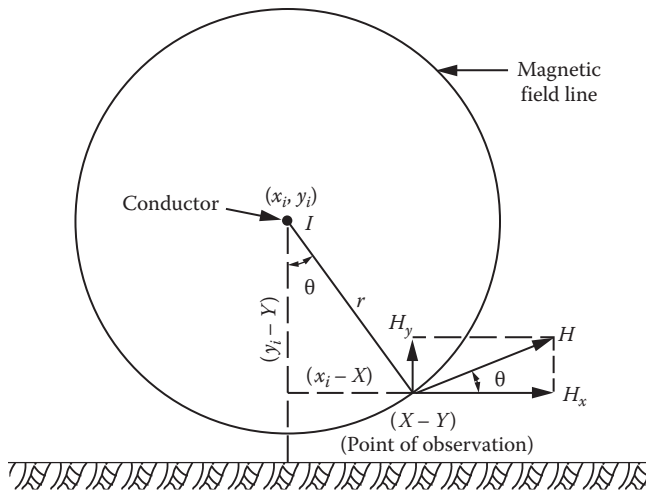


Figure 2.80 Magnetic field generation by a current-carrying conductor.

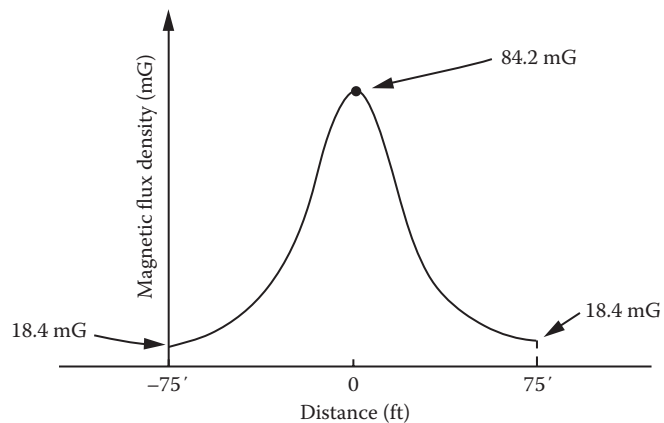


Figure 2.81 Magnetic field density distribution.

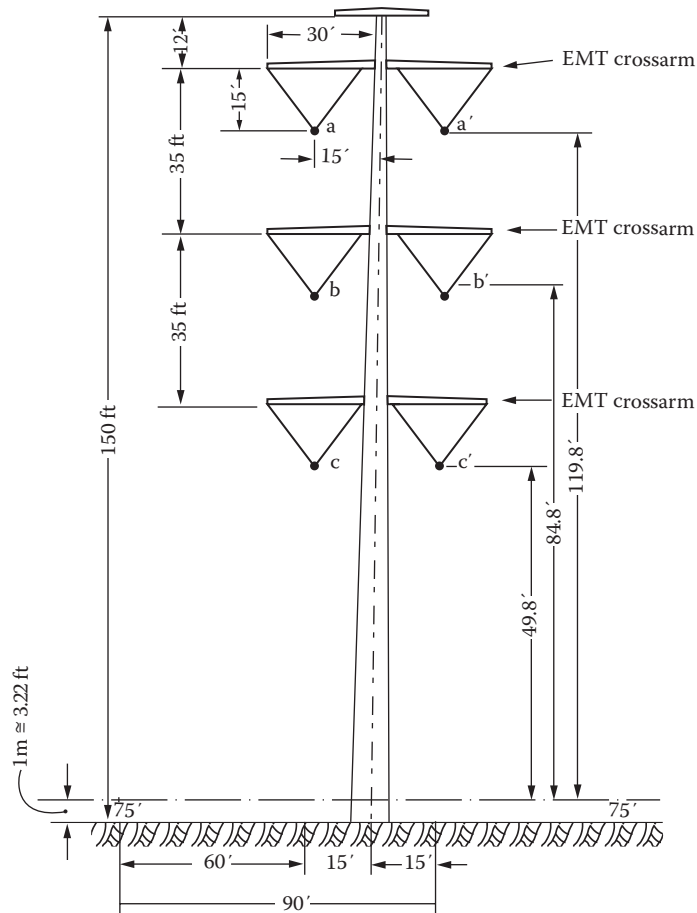


Figure 2.82 A typical tower used in Example 2.4.

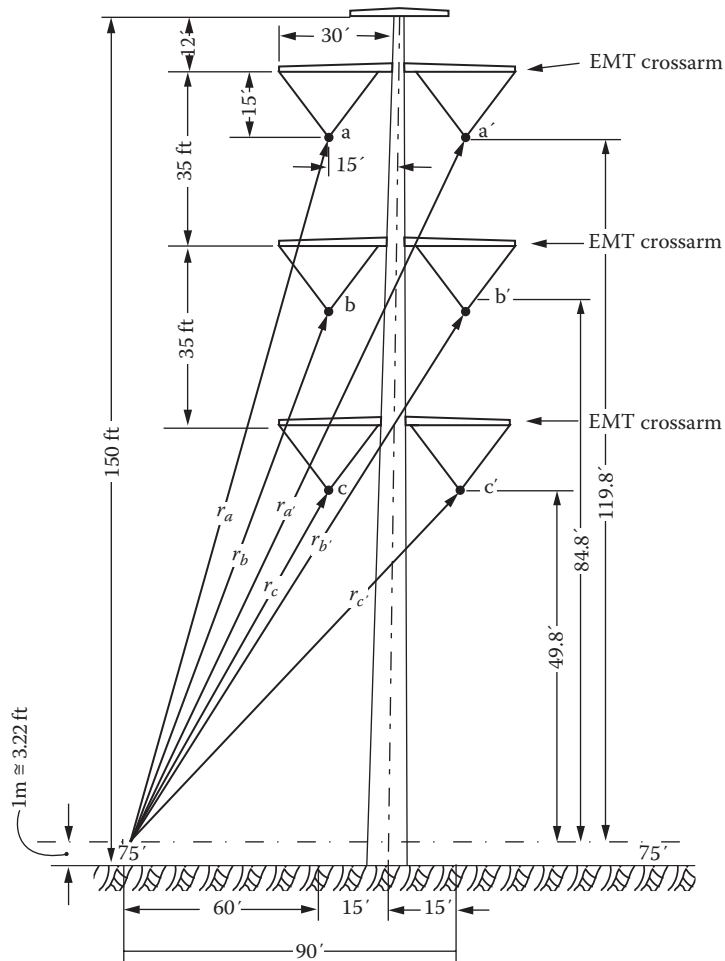


Figure 2.83 The radiuses in question in terms of the geometry involved with respect to the edge of the ROW.

